Localization of the Seizure Focus

Box 97.1 The International League Against Epilepsy (ILEA) classification of seizures

I. Partial (focal) seizures

A. Simple partial seizures (consciousness not impaired)
B. Complex partial seizures (with impairment of consciousness)
C. Partial seizures evolving to secondarily generalized seizures

II. Generalized seizures (convulsive or non-convulsive)

A. Absence seizures
B. Myoclonic seizures
C. Clonic seizures
D. Tonic seizures
E. Tonic–clonic seizures
F. Atonic seizures

III. Unclassified seizures

Partial seizures

Partial seizures have a focal origin and are therefore most suitable for surgical treatment by brain resection

Complex partial seizures

Complex partial seizures are those of focal origin in which consciousness is impaired

Complex partial seizures

The majority of complex partial seizures arise from the temporal lobes but they can arise from other cortical areas

Complex partial seizures

Over 40% of patients with complex partial seizures are not adequately controlled with medication and are termed refractory or intractable

One of the most effective treatments for partial epilepsy, refractory to medical intervention, is surgical removal of the involved area.

Pre-surgical localization of the seizure focus

- EEG
  - Scalp EEG
  - Sphenoidal leads
  - Subdural and epidural electrodes and grids
  - Depth electrodes
- Structural imaging
  - CT
  - MRI
- Physiological imaging
  - SPECT (Single Photon Emission Computed Tomography)
    - Blood flow, Tc-99m HMPAO
  - PET (Positron Emission Tomography)
    - Metabolism , FDG

5.2 RADIOPHARMACEUTICALS

Table 5.1 Radiopharmaceuticals for brain imaging

Radiotracer	Site localization	Pathological localization	Agent of choice in investigation of:
Blood–brain barrier agents			
$^{99m}TcO_4$ ^{99m}Tc DTPA ^{99m}Tc GHA	Localize in the intravascular space	Localize in regions where BBB breakdown occurs. Show abnormal blood pools	Primary and secondary brain tumours Herpes encephalitis Subdurals Carotid stenosis AVMs
Cerebral perfusion agents			
^{99m}Tc HMPAO ^{123}I IMP ^{99m}Tc ECD	Taken up by the brain	Decreased uptake seen in areas of hypoperfusion or hypofunction	Cerebral infarction and haemorrhage TIAs Epilepsy Dementia Head trauma
CSF agents			
^{111}In DTPA ^{99m}Tc DTPA	Remain in CSF	Enter abnormally dilated ventricles communicating with CSF. Show abnormal CSF dynamics, leaks and shunts	Dilated ventricles CSF leaks Shunt patency
Tumour agents			
^{201}Tl	Extracellular fluid	Tumours	Tumour recurrence vs fibrosis/necrosis

DTPA, diethylenetriamine pentaacetic acid; GHA, glucoheptonate; HMPAO, hexamethylpropyleneamine oxime; IMP, iodoamphetamine; ECD, ethyl cysteinate dimer

Cerebral perfusion agents

- Lipophilic radiopharmaceuticals
- Cross the intact blood-brain barriers and are retained by the brain tissue in proportion to regional cerebral blood flow (rCBF)
- Map the distribution in both normal and pathologic brain tissue

Tc-99m HMPAO (hexamethyl-propyleneamineoxime)

- Small and highly lipophilic molecules
- Cross the BBB in proportion to blood flow

↓

It is rapidly converted to a less-lipophilic form, becomes trapped in the brain and remains in a stable distribution for many hours

↓

Thus a “freeze-frame” image of blood flow corresponding to the time of injection can be imaged several hours later

Seizure foci

- During seizures (ictal studies)

  Hyperperfusion

- Between seizures (interictal studies)

  Hypoperfusion

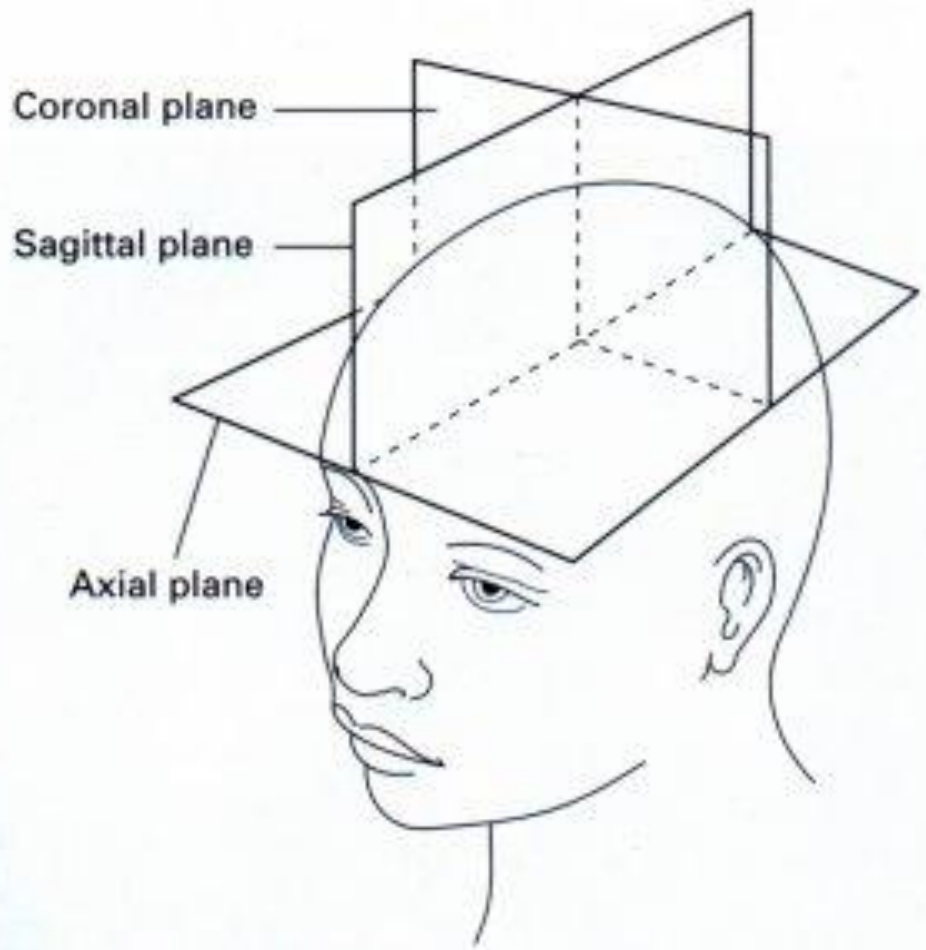

Fig. 15.13 Illustration of the axial, coronal and sagittal planes.

Interictal studies

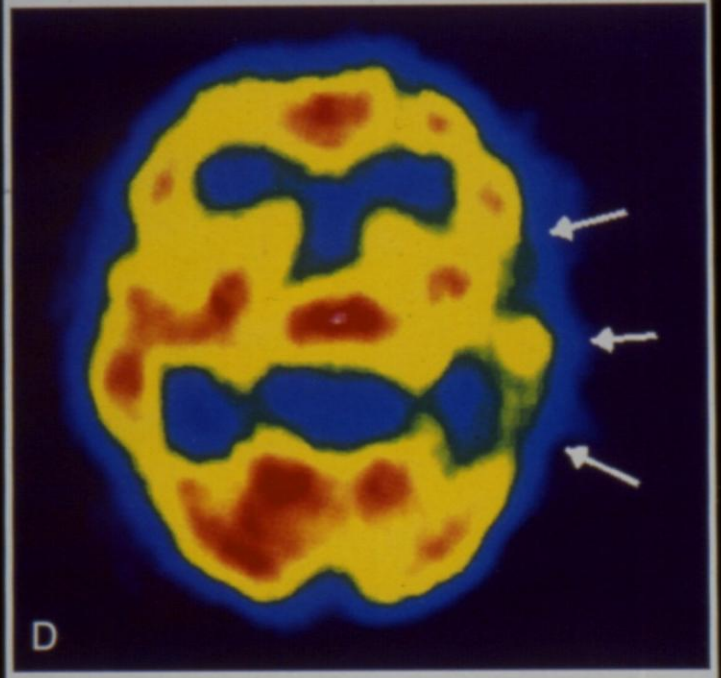

D

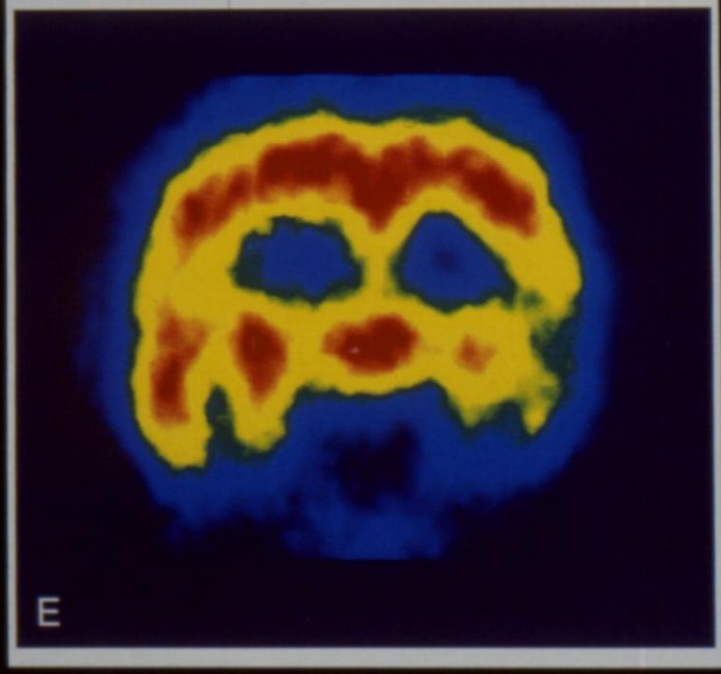

E

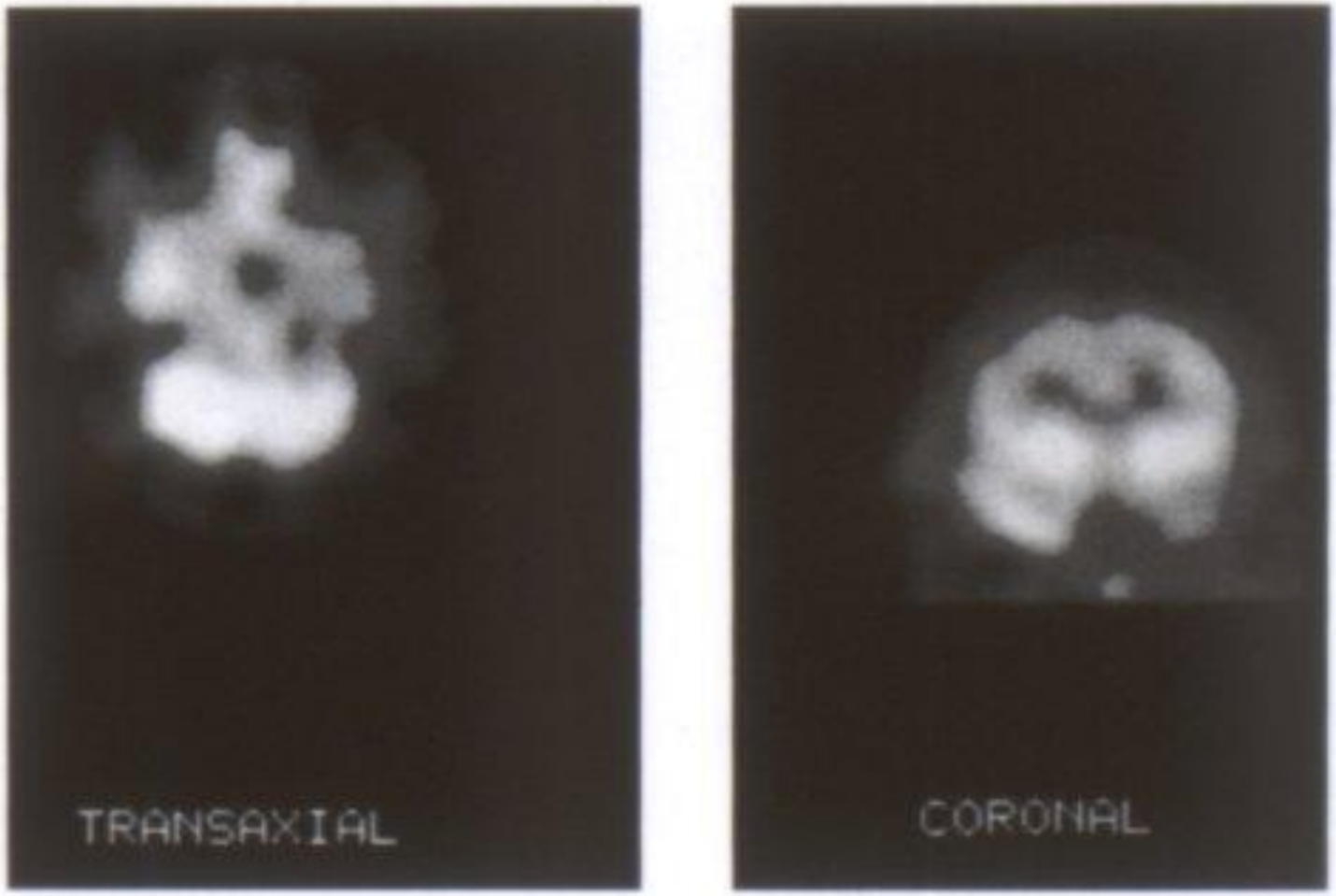

FIG. 10-5. Interictal SPECT cerebral perfusion examination using HMPAO in a patient with medically intractable partial complex epilepsy. The selected transaxial and coronal planes demonstrate hypoperfusion of the left temporal lobe.

Ictal studies

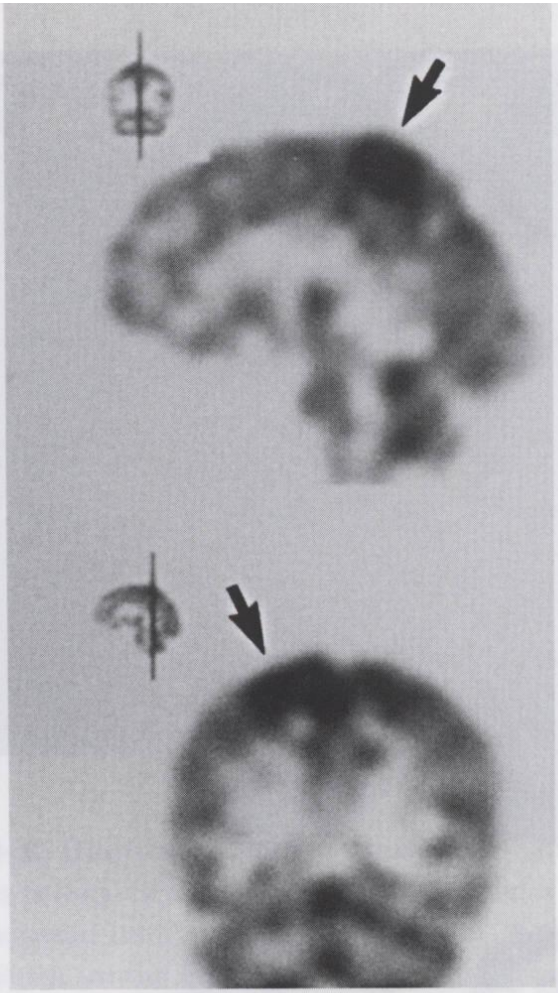

FIGURE 4–10. Epilepsy (ictal). Sagittal and coronal SPECT brain perfusion images obtained with the radiopharmaceutical ^{99m}Tc-HMPAO during seizure show markedly increased activity in the right parietal cortex (*arrows*), indicating increased perfusion of the epileptogenic focus. (Case courtesy of B. Barron, M.D., and Lamk Lamki, M.D.)

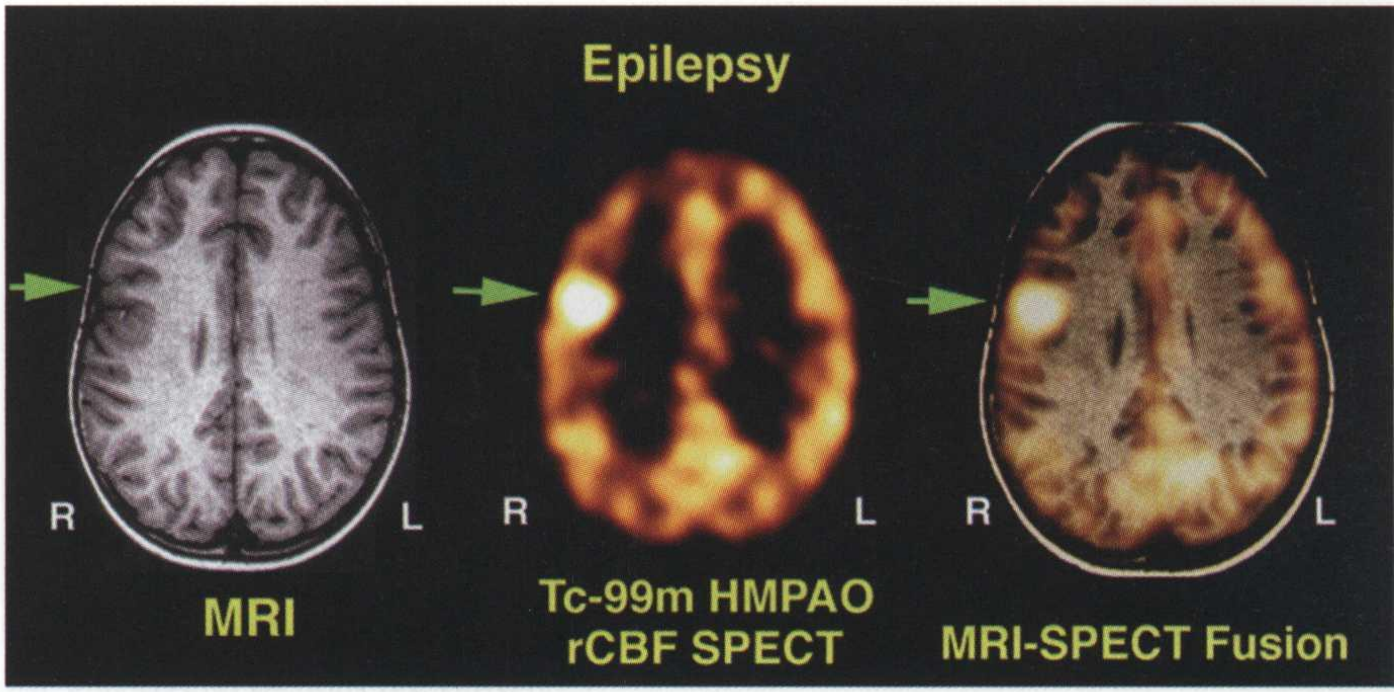

Fig. 18.25. Frontal lobe epilepsy in a 9-year-old right-handed boy. The MRI scan (*left*) is normal. The Tc-99m-HMPAO brain SPECT scan (*middle*) reflects the regional cerebral perfusion at the time the tracer was injected during the epileptogenic seizure. The intense region of hyperemia is seen at the 10 o'clock position. A SPECT MRI fusion image (*right*) clearly identifies the location of the focus on the MRI scan

In general, ictal studies are more sensitive in the detection of seizure foci than are interictal studies, with a sensitivity of 85% to 95% ictally and of about 70% interictally

Positron Emission Tomography (PET)

POSITRON

A positively charged electron

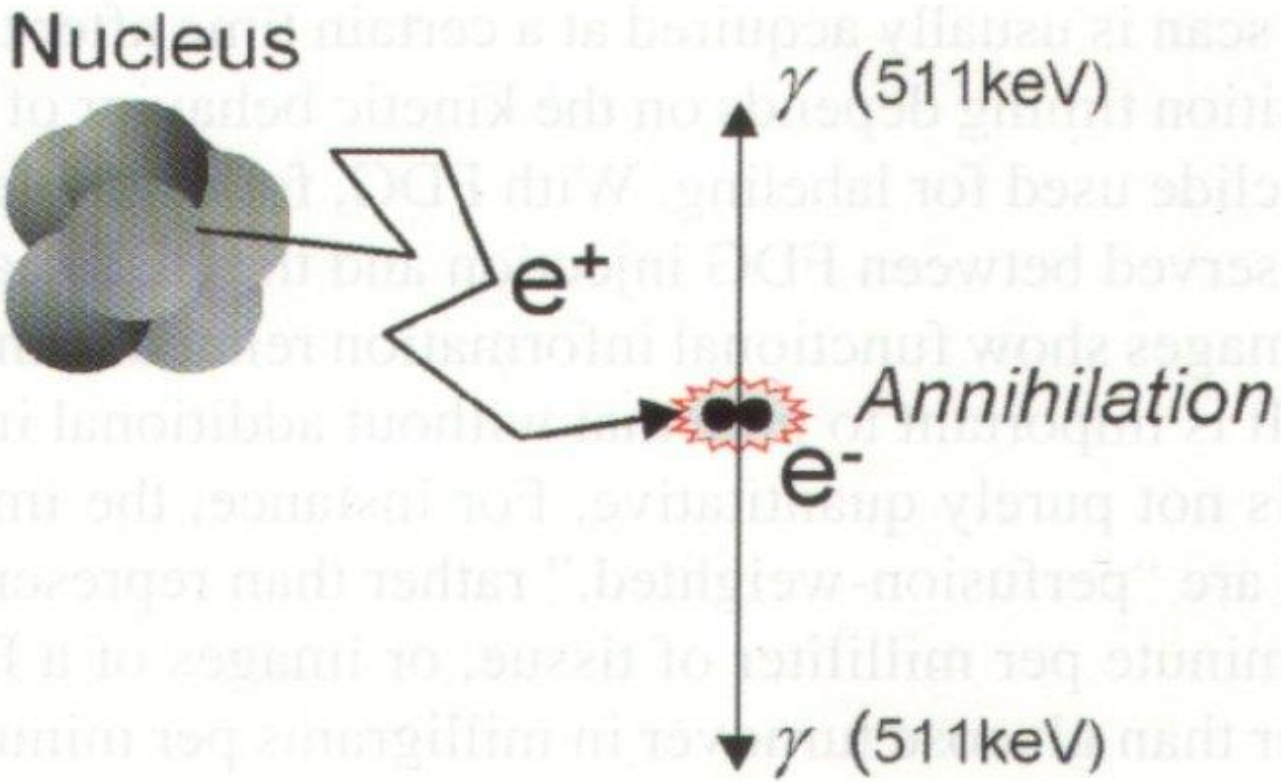

Figure 2-1. Physical effect used in PET imaging. A positron is emitted from the nucleus, is slowed down, and finally interacts with an electron in an annihilation process. The masses are converted in two 511-keV photons that travel in opposite directions.

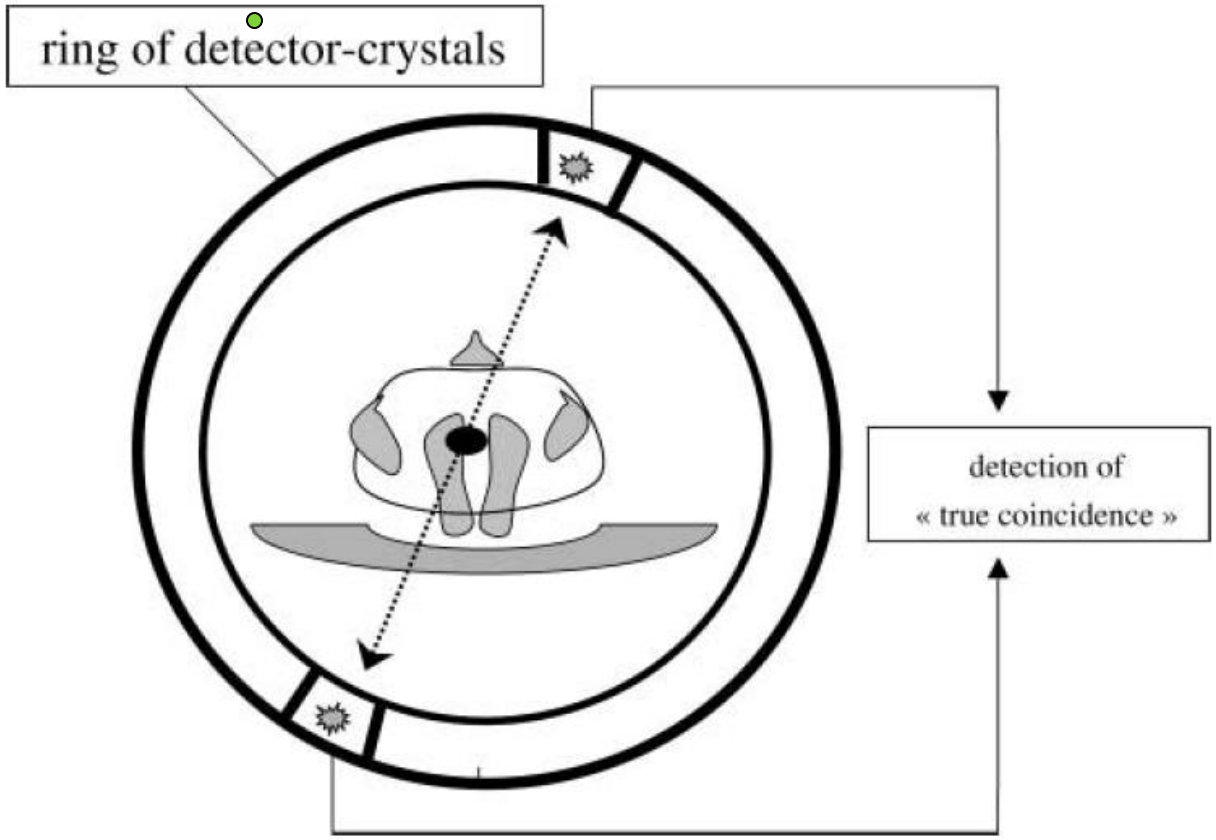

Fig. 1 Schematic presentation of the PET scanner and the "coincidence detection" process

Fluorine-18 Fluorodeoxyglucose (^{18}F-FDG)

- Is an analog of glucose and is used as a tracer of glucose metabolism
- The most commonly used positron-emitting radiopharmaceutical in clinical imaging

FDG

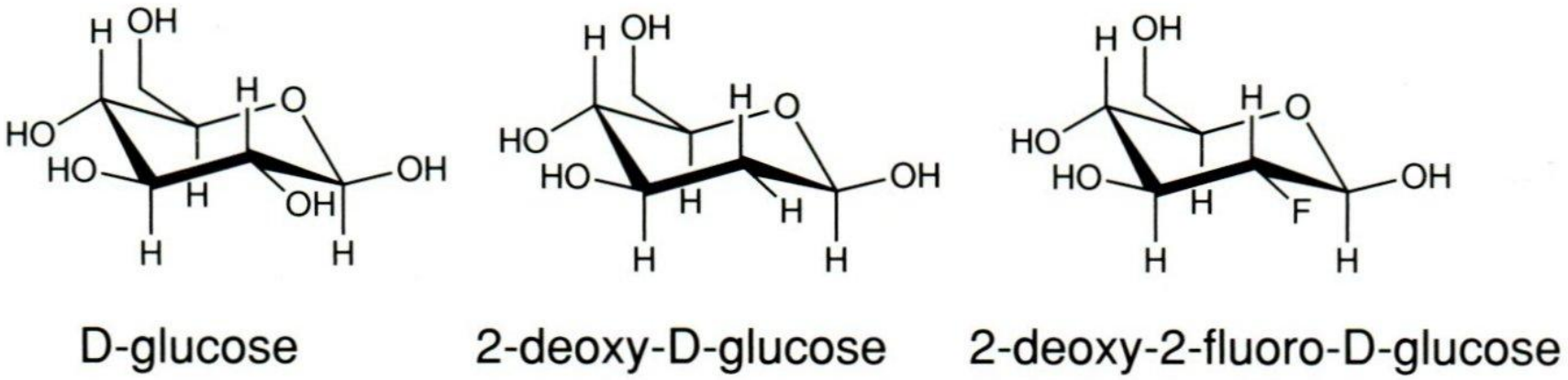

FIGURE 2.3. Structures of glucose, 2-deoxy-D-glucose and 2-deoxy-2-fluoro-D-glucose.

Seizure foci

- During seizures (ictal studies), not done

  Hypermetabolism

- Between seizures (interictal studies)

  Hypometabolism

Ictal PET studies

Performing ictal PET studies is somewhat impractical because of the short half-life of the positron emitters and other logistic reasons

Ictal PET studies

Since the FDG uptake phase lasts up to 20-40 min after injection, the seizure focus may be a mixture of ictal (increased uptake) and peri-ictal (decreasing uptake) finding.

Interictal PET studies

Hypometabolism in the seizure focus, similar to the

hypoperfusion seen with SPECT brain perfusion agents

Interictal study

MRI

PET

PET/MRI

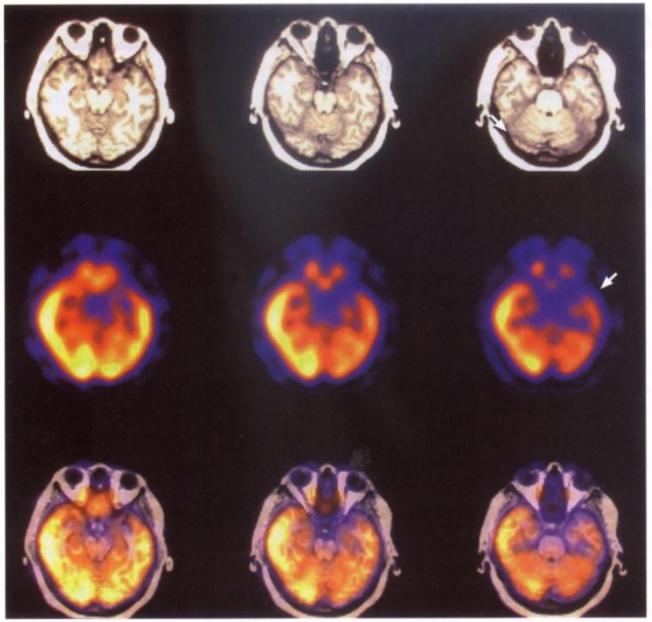

A

MRI

PET

PET/MRI

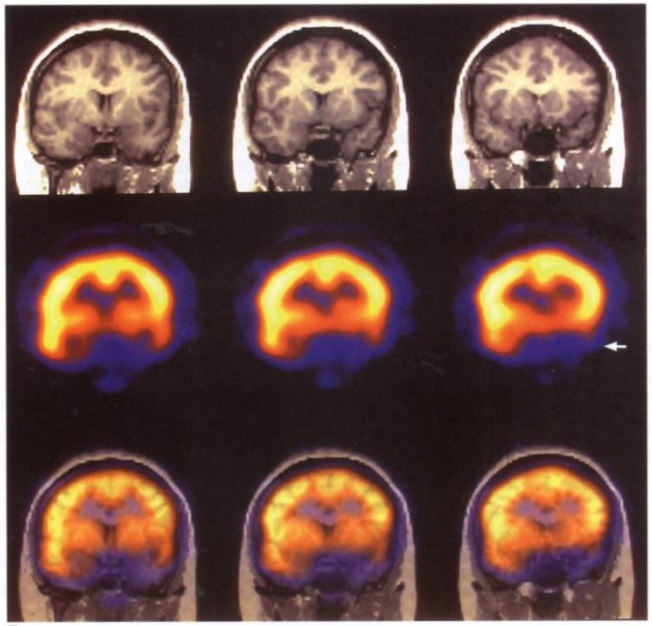

B

FIGURE 13–25. Epilepsy interictal study. Transaxial (*A*) and coronal (*B*) magnetic resonance imaging (MRI) (*upper row*), ^{18}F-FDG PET images (*middle row*), and PET/MRI fusion images (*lower row*) show an area of decreased metabolism in the left temporal lobe (*arrows*).

SPECT
ictal

PET
interictal

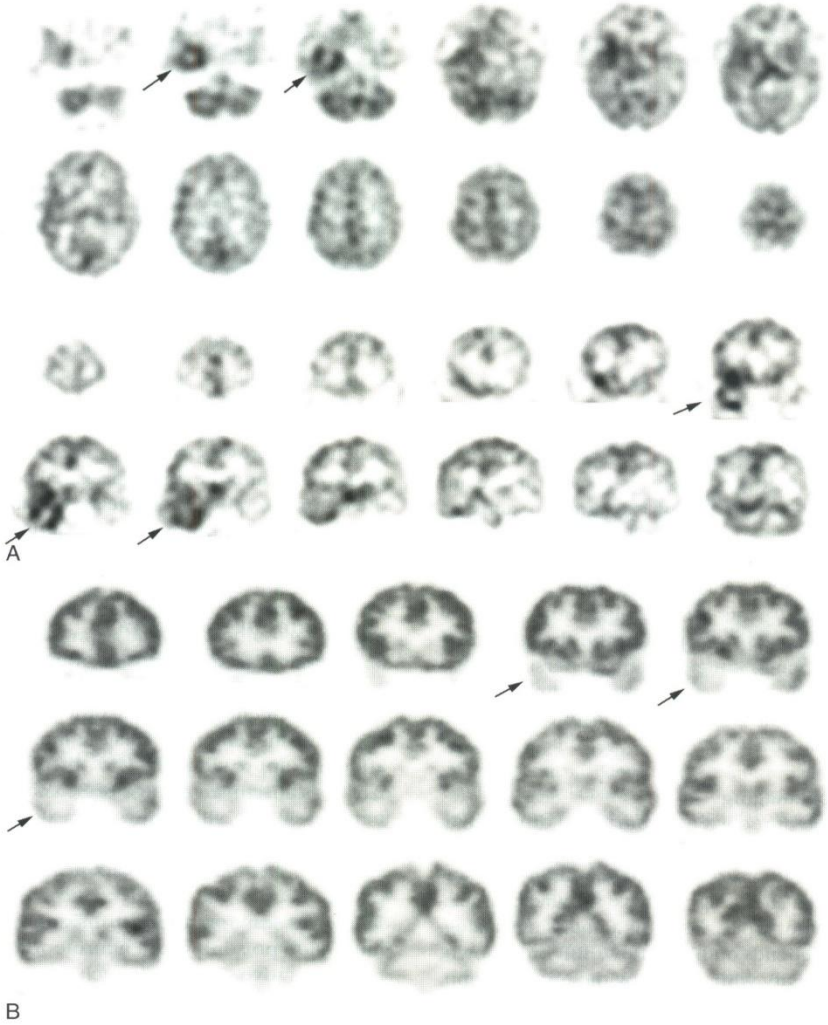

SPECT
ictal

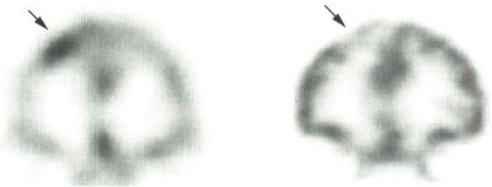

PET
interictal

Figure 13-19 Seizure imaging. **A,** Ictal HMPAO SPECT axial (*top*) and coronal (*bottom*) images reveal increased perfusion to the right temporal region from an active seizure. **B,** The abnormal temporal region is a subtle area of hypometabolism on the Interictal FDG PET. **C,** A second patient ictal SPECT demonstrates hyperperfusion in the right parasagittal region (*left*) which is an area of hypometabolism on interictal PET (*right*) from a seizure focus.

Alzheimer’s Disease

TABLE 132-2. Causes of Dementia in Adults

- Degenerative disorders
  - Alzheimer's disease
  - Pick's disease
  - Nonspecific neuron loss
  - Parkinson's disease
  - Diffuse Lewy body disease
  - Huntington's disease
  - Progressive supranuclear palsy
  - Spinocerebellar degenerations
  - Idiopathic basal ganglia calcification
  - Striatonigral degeneration
  - Wilson's disease
  - Hallervorden-Spatz disease
  - Thalamic dementia
  - Motor neuron disease
- Vascular dementias
  - Multiple large vessel occlusions
  - Lacunar state (multiple subcortical infarcts)
  - Binswanger's disease
  - Mixed cortical/subcortical infarctions
  - Mitochondrial encephalomyopathies
- Myelinoclastic disorders
  - Demyelinating
    - Multiple sclerosis
    - Marchiafava-Bignami disease
  - Dysmyelinating
    - Metachromatic leukodystrophy
    - Adrenoleukodystrophy
    - Cerebrotendinous xanthomatosis
    - Ceroid lipofuscinosis (Kufs disease)
    - Polyglucosan body disease
    - Tay-Sachs disease
- Traumatic conditions
  - Subdural hematoma
  - Dementia pugilistica
- Neoplastic dementias
  - Meningioma (particularly subfrontal)
  - Glioma
  - Metastatic lesions
  - Meningeal carcinomatosis
  - Paraneoplastic
- Hydrocephalic dementias
  - Communicating
    - Normal pressure hydrocephalus
  - Noncommunicating
    - Aqueductal stenosis
    - Intraventricular neoplasm
    - Intraventricular cyst
    - Basilar meningitis
- Inflammatory conditions
  - Systemic lupus erythematosus
  - Temporal arteritis
  - Sarcoidosis
  - Sjögren-Larsson syndrome
  - Granulomatous arteritis
- Infection-related dementias
  - Syphilis
  - Lyme disease
  - Chronic meningitis (tuberculosis, fungal)
  - Brain abscess
  - Progressive multifocal leukoencephalopathy
  - Whipple's disease
  - Human immunodeficiency virus encephalopathy/opportunistic infections
  - Creuzfeldt-Jakob disease
  - Gerstmann-Straussler disease
  - Subacute sclerosing panencephalitis
- Metabolic disorders
  - Cardiopulmonary failure—hypoxia, hypercapnia
  - Uremia
  - Hepatic encephalopathy
  - Endocrine disorders
    - Thyroid
    - Adrenal
    - Parathyroid
  - Anemia and other hematologic conditions
  - Deficiency states (vitamin B_{12}, folate, niacin)
  - Porphyria
  - Hypoglycemia
- Toxic exposures
  - Alcohol-related syndromes
  - Polydrug abuse
  - Heavy metals
  - Industrial solvents
- Psychiatric disorders
  - Depression
  - Mania
  - Schizophrenia
  - Conversion reaction
  - Malingering

Box 12-9 Causes of Dementia

DISEASE	INCIDENCE (%)
Alzheimer's disease	50-60
Parkinsonism	15
Multiinfarct dementia	5-10
Drugs and alcohol	10
Pick's disease	<1
Creutzfeldt-Jakob disease	<1
Progressive supranuclear palsy	<1
Huntington's chorea	<1
Multiple sclerosis	<1
Vitamin B_{12} deficiency	<1
Endocrine (hypothyroid) disease	<1
Chronic infection (e.g., tuberculosis, syphilis)	<1
Human immunodeficiency virus encephalopathy	

5.2 RADIOPHARMACEUTICALS

Table 5.1 Radiopharmaceuticals for brain imaging

Radiotracer	Site localization	Pathological localization	Agent of choice in investigation of:
Blood–brain barrier agents			
$^{99m}TcO_4$ ^{99m}Tc DTPA ^{99m}Tc GHA	Localize in the intravascular space	Localize in regions where BBB breakdown occurs. Show abnormal blood pools	Primary and secondary brain tumours Herpes encephalitis Subdurals Carotid stenosis AVMs
Cerebral perfusion agents			
^{99m}Tc HMPAO ^{123}I IMP ^{99m}Tc ECD	Taken up by the brain	Decreased uptake seen in areas of hypoperfusion or hypofunction	Cerebral infarction and haemorrhage TIAs Epilepsy Dementia Head trauma
CSF agents			
^{111}In DTPA ^{99m}Tc DTPA	Remain in CSF	Enter abnormally dilated ventricles communicating with CSF. Show abnormal CSF dynamics, leaks and shunts	Dilated ventricles CSF leaks Shunt patency
Tumour agents			
^{201}Tl	Extracellular fluid	Tumours	Tumour recurrence vs fibrosis/necrosis

DTPA, diethylenetriamine pentaacetic acid; GHA, glucoheptonate; HMPAO, hexamethylpropyleneamine oxime; IMP, iodoamphetamine; ECD, ethyl cysteinate dimer

The scintigraphic appearance of Alzheimer's disease

Bilateral hypoperfusion in posterior temporal and/or parietal regions

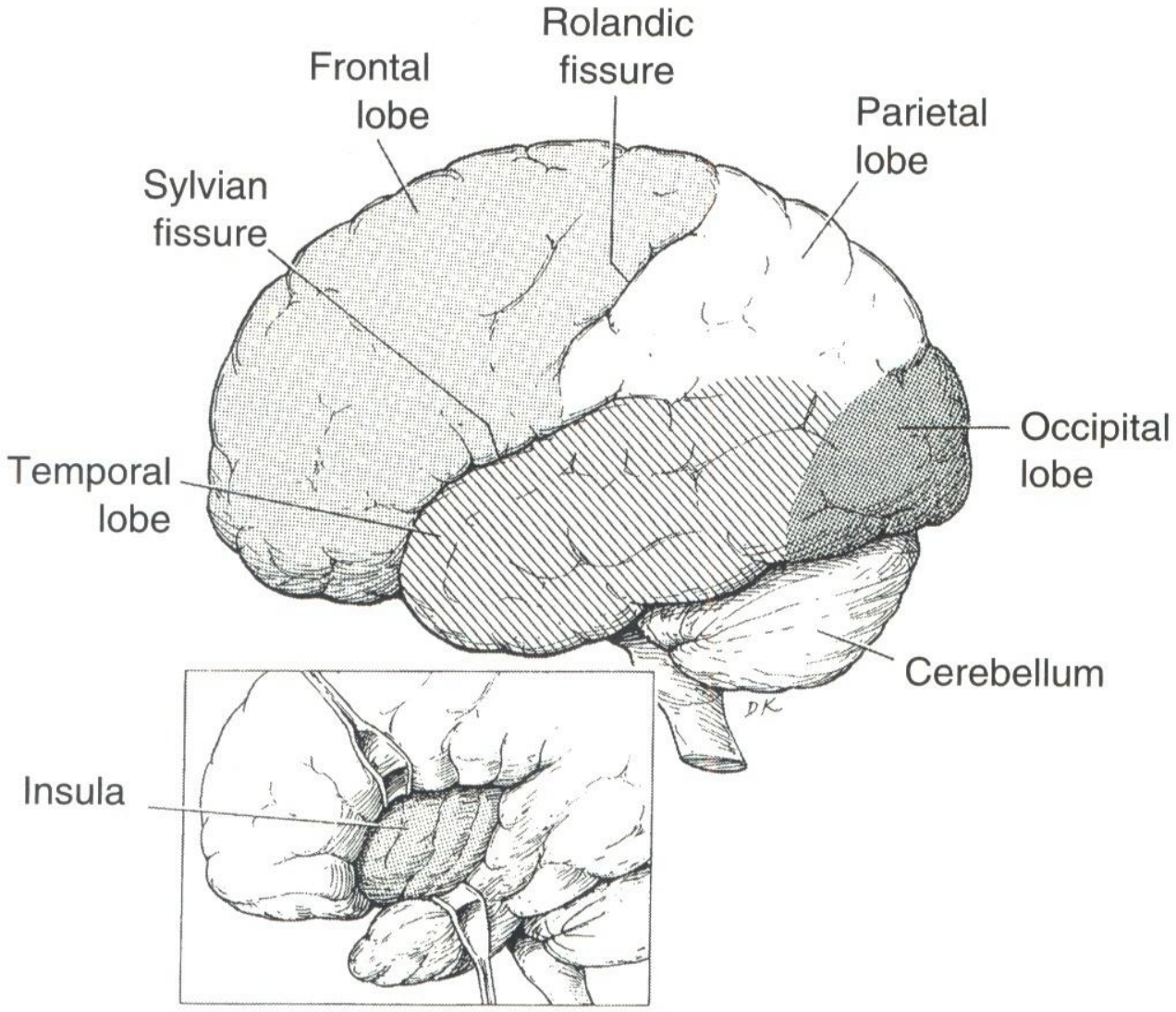

Figure 13-1 Cerebral cortex lobar anatomy.

ALZHEIMER'S TYPE DEMENTIA

Patient 1

FIGURE 62–14 A and B.

Transverse ^{99m}Tc-HMPAO SPECT Scan: There is decreased perfusion *(arrows)* to both parietal lobes and the posterior temporal lobes. There is also mild frontal lobe hypoperfusion.

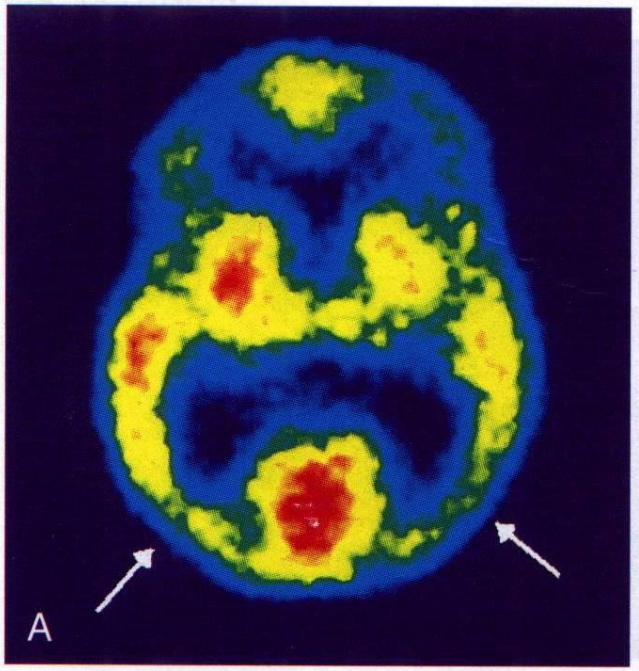

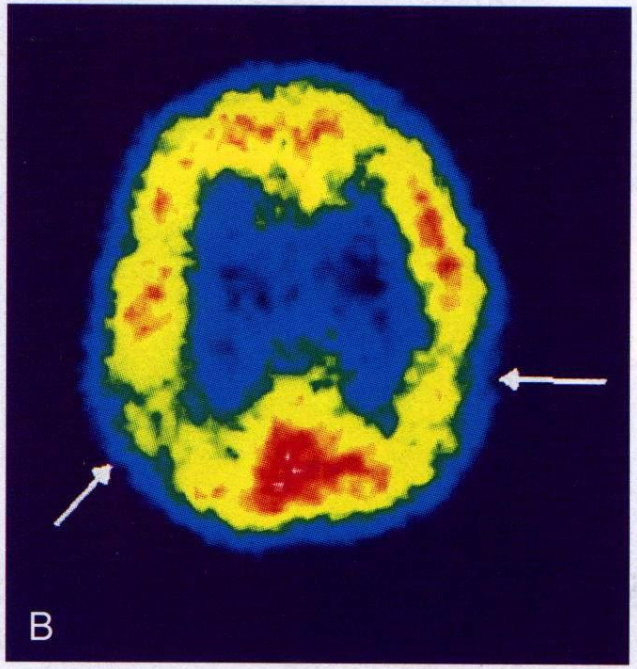

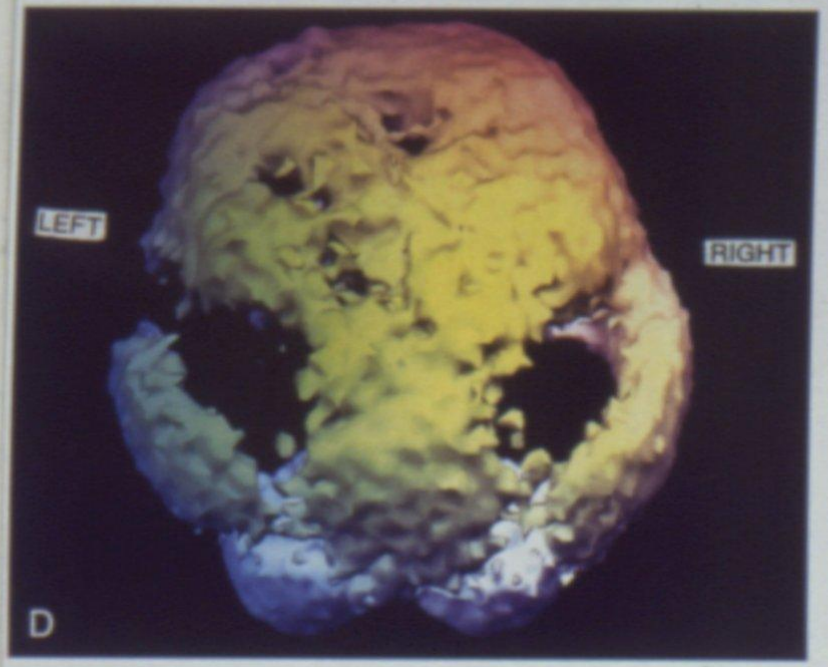
LEFT
RIGHT
D

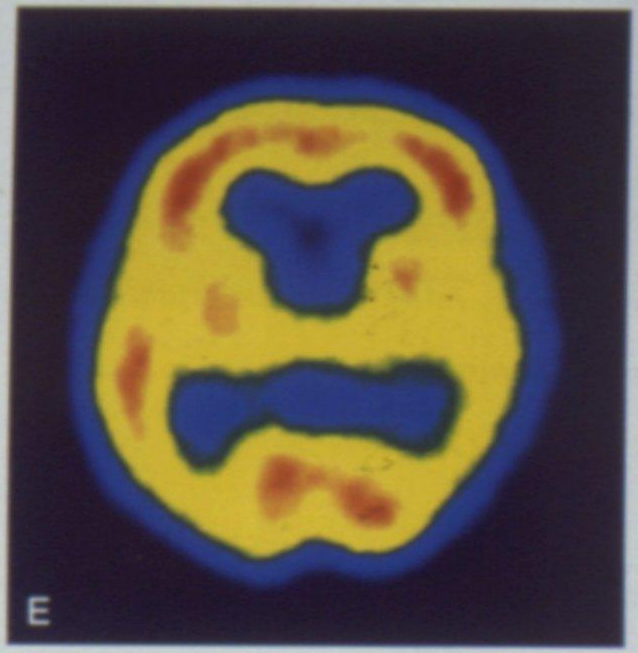
E

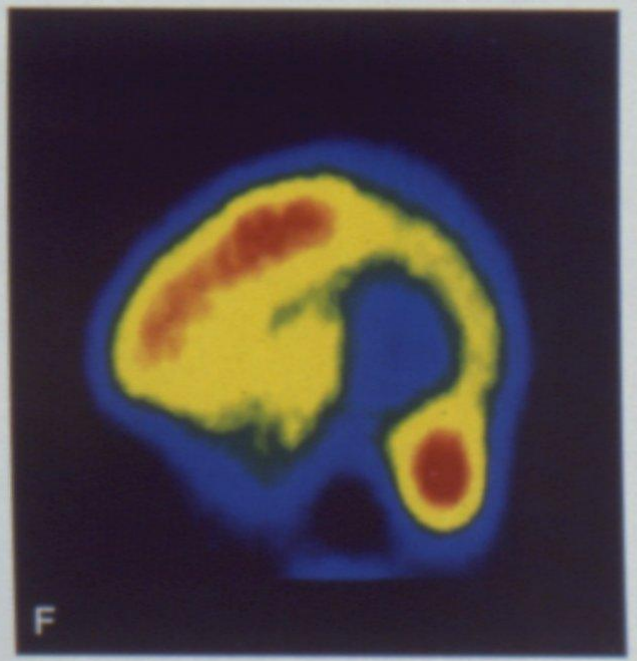
F

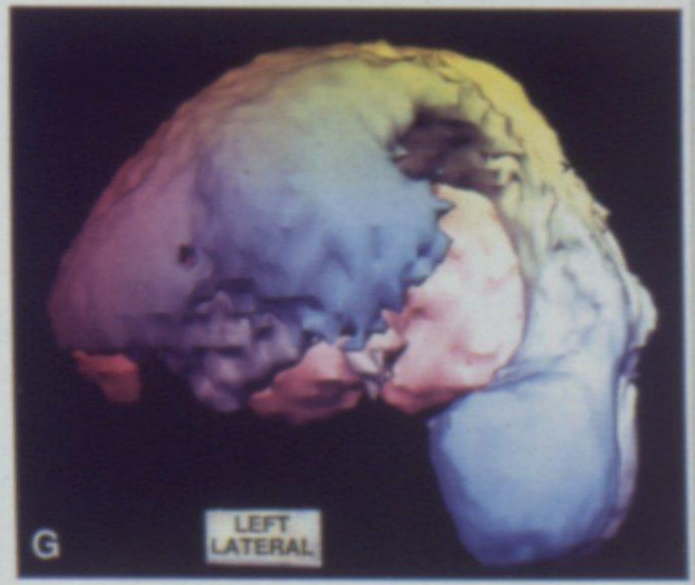
LEFT
LATERAL
G

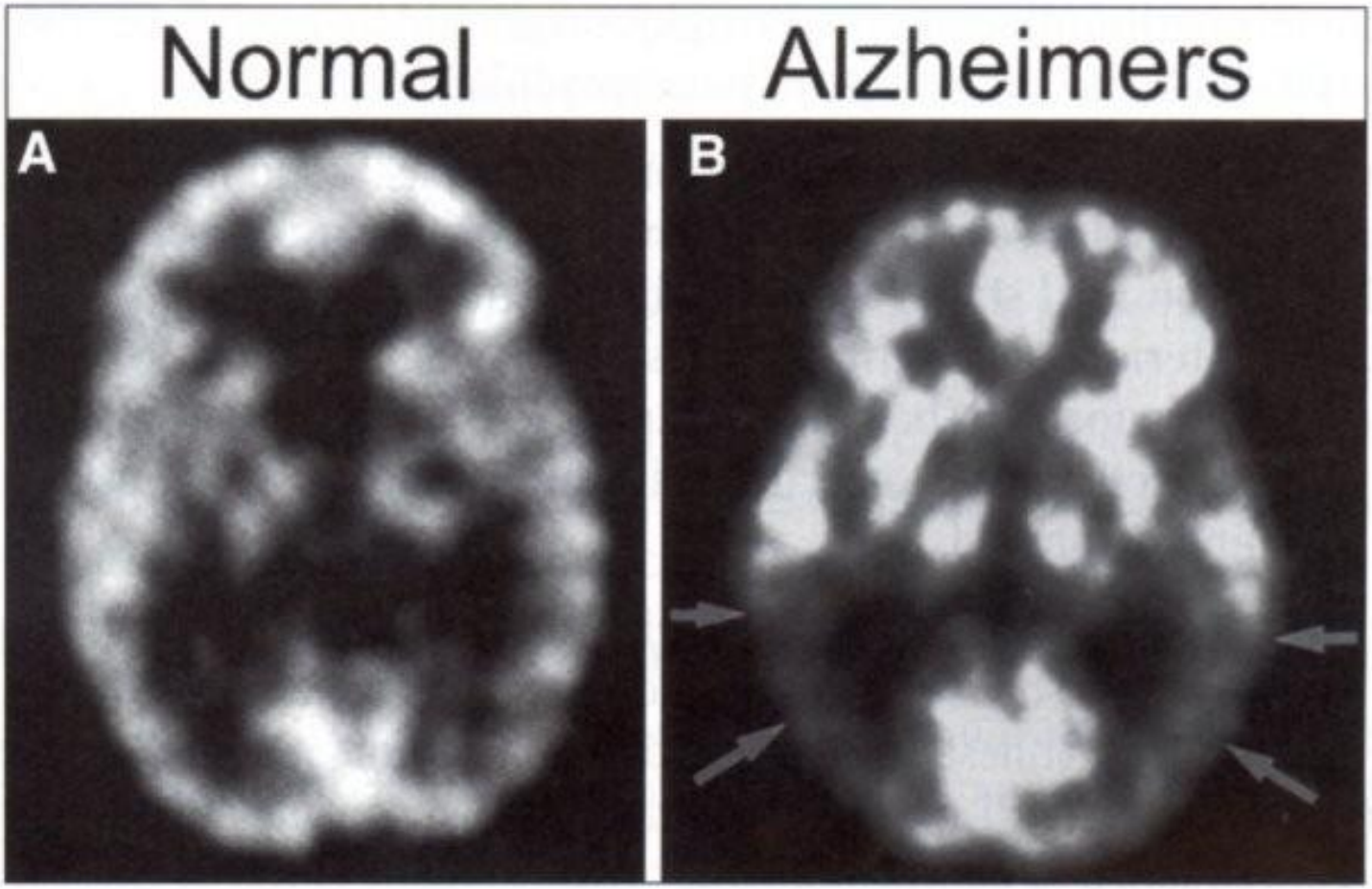

Figure 1. Single axial slice from a normal brain (A), contrasted with a patient with Alzheimer's dementia (B). Note relative decreased perfusion in the Alzheimer's brain in the parietal and temporal lobes (arrows).

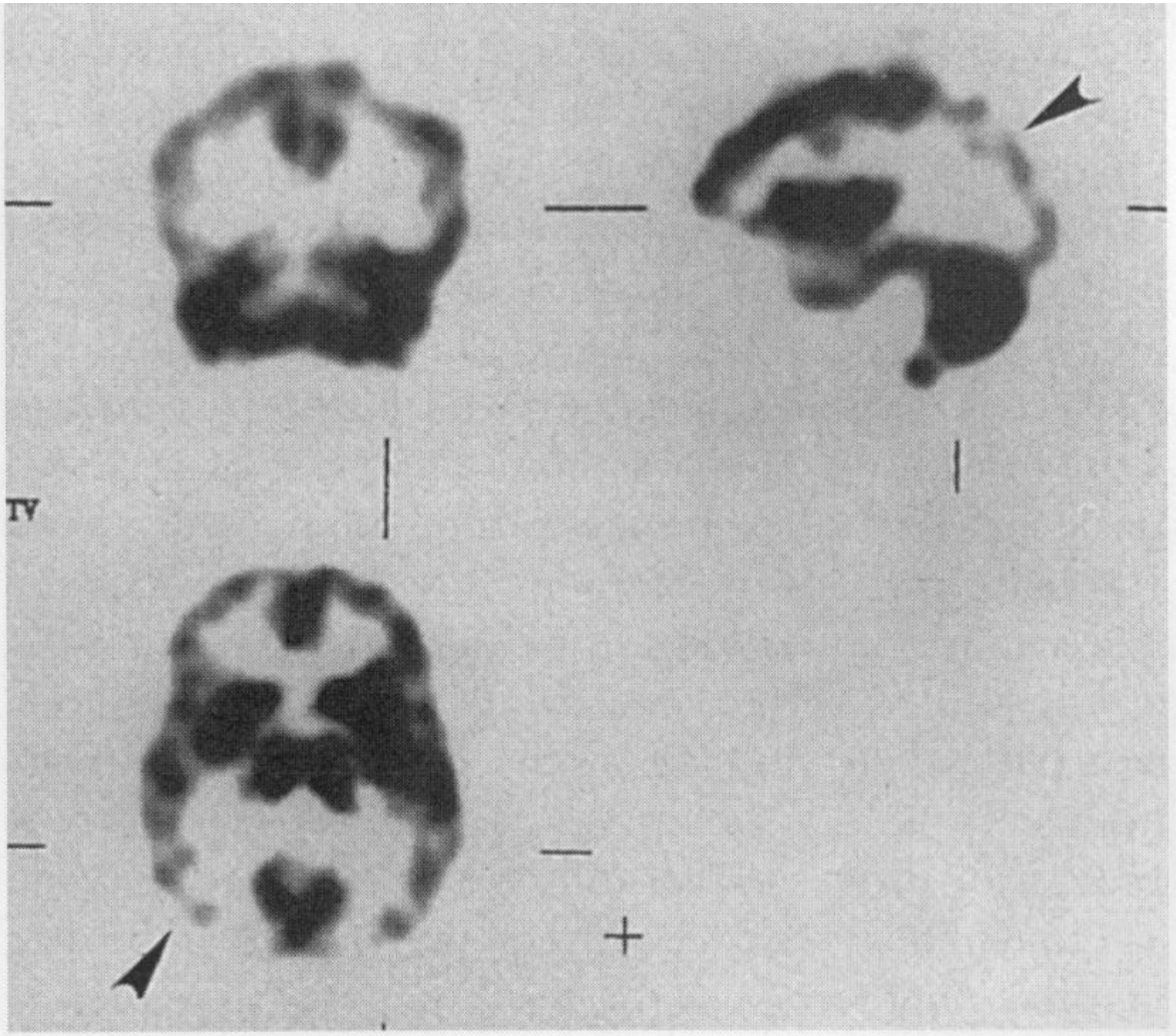

Fig. 12-19 Alzheimer's disease. The patient had dementia, and Alzheimer's disease was clinically suspected. The three-view display of selected coronal, sagittal, and transverse technetium-99m HMPAO sections shows a classic pattern of Alzheimer's disease with bilateral temporal-parietal hypoperfusion *(arrowheads)*. This is best seen in the sagittal view.

FDG-PET, Dementia

In dementia, metabolic distribution patterns demonstrated on FDG-PET scans are broadly comparable to those seen by using SPECT brain perfusion agents, generally with greater sensitivity and overall accuracy.

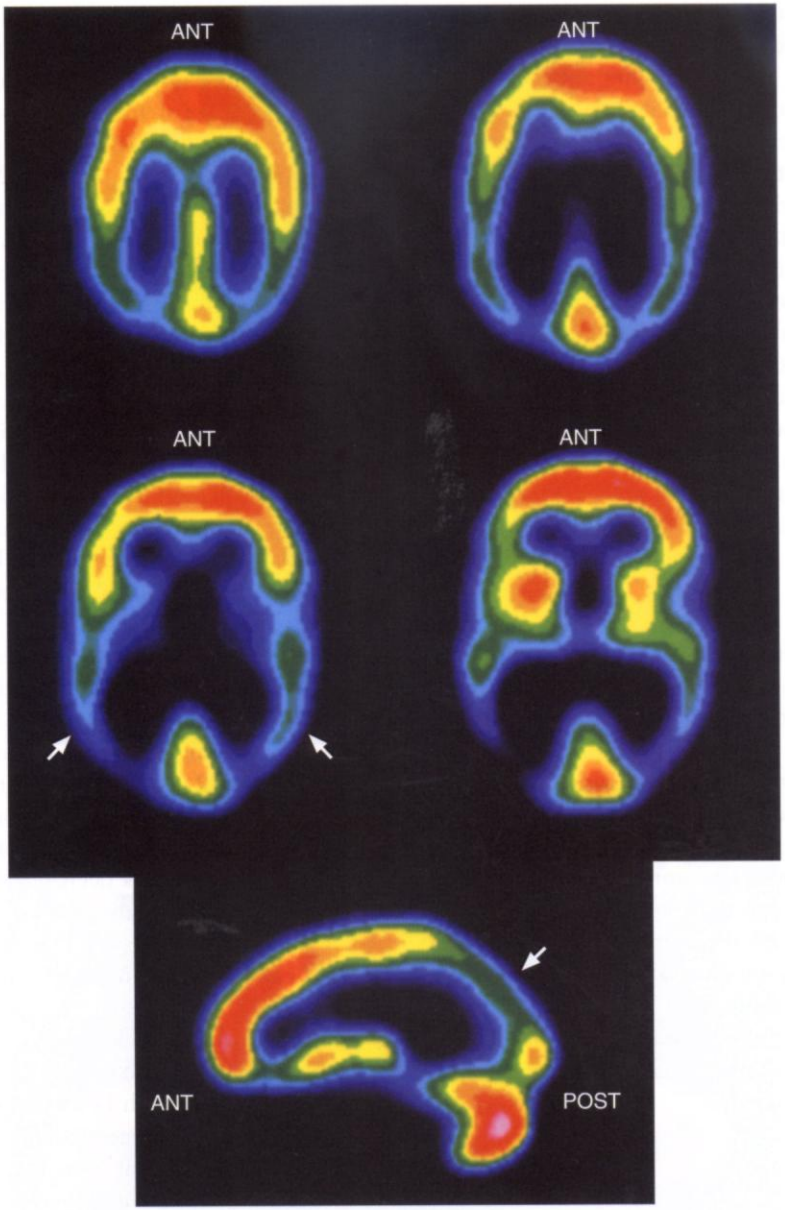

FIGURE 13–27. Alzheimer's dementia. Multiple transaxial and one sagittal image from a ^{18}F-FDG PET scan show symmetrically decreased metabolic activity in the posterior tempoparietal regions (*arrows*).

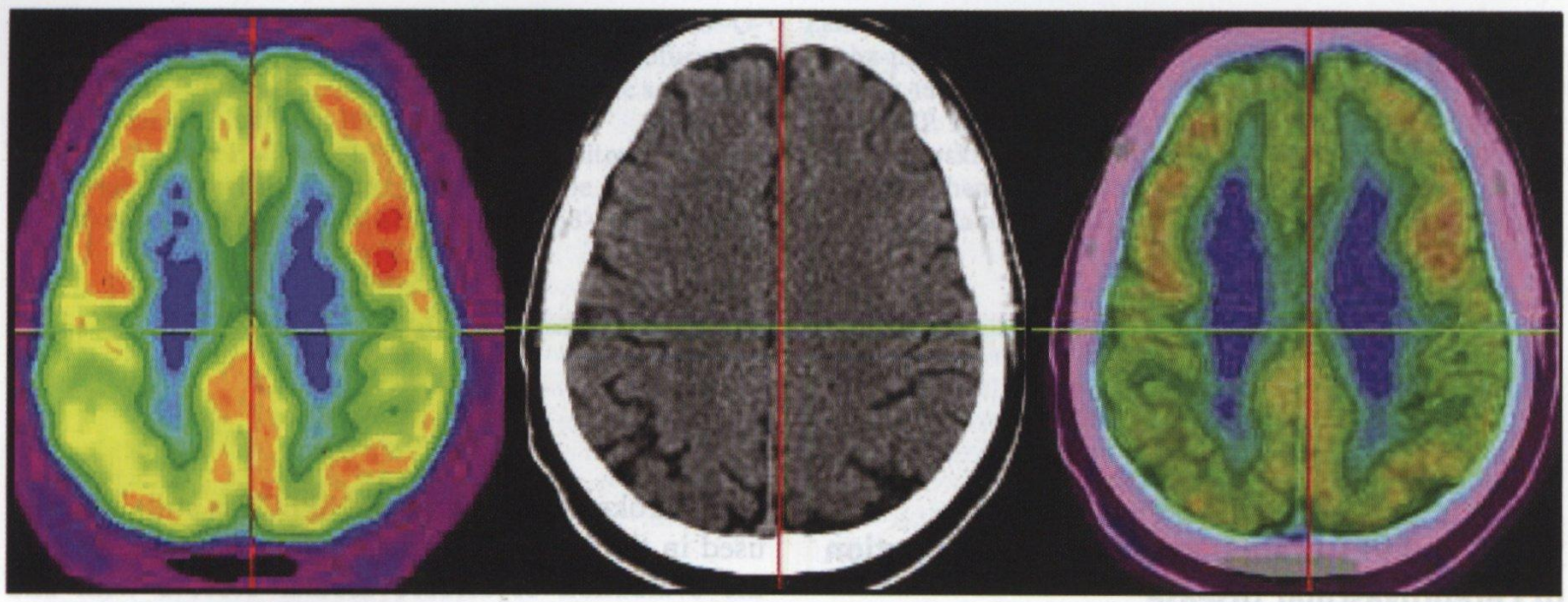

Fig. 3.2. The value of PET/CT in the evaluation of Alzheimer's disease – transverse plane FDG-PET (*left*), CT (*middle*) and fused PET/CT (*right*) images. Study reveals evidence of bilateral posterior parietal hypometabolism without evidence of significant cortical atrophy on CT

Radionuclide Shuntogram

Hydrocephalus in adults

Hydrocephalus

- Hydrocephalus is enlargement of the ventricular cavities with a pathological increase in CSF volume
- Occurs after an imbalance between CSF formation and absorption

Table 12-4 Classification of hydrocephalus

Classification	Site of obstruction	Scintigraphy type
OBSTRUCTIVE		
Noncommunicating	Intraventricular, between lateral ventricles and basal cisterns	I, II
Communicating	Extraventricular, affecting basal cisterns, cerebral convexities, and arachnoid villi	IIIA, IIIB, IV
NONOBSTRUCTIVE		
Generalized	Cerebral atrophy	II
Localized	Porencephaly	

- Non-communicating hydrocephalus

  Obstruction within the ventricular system or at the outlet of the 4th ventricle

- Communicating hydrocephalus

  CSF can flow freely from the ventricles to the subarachnoid space

  (obstruction in the subarachnoid space)

Treatment

- There is no satisfactory medical treatment for hydrocephalus.
- The usual surgical treatment option is placement of a CSF shunt

Shunt placement for CSF diversion

Allowing drainage of excess fluid

to a terminal reabsorption site

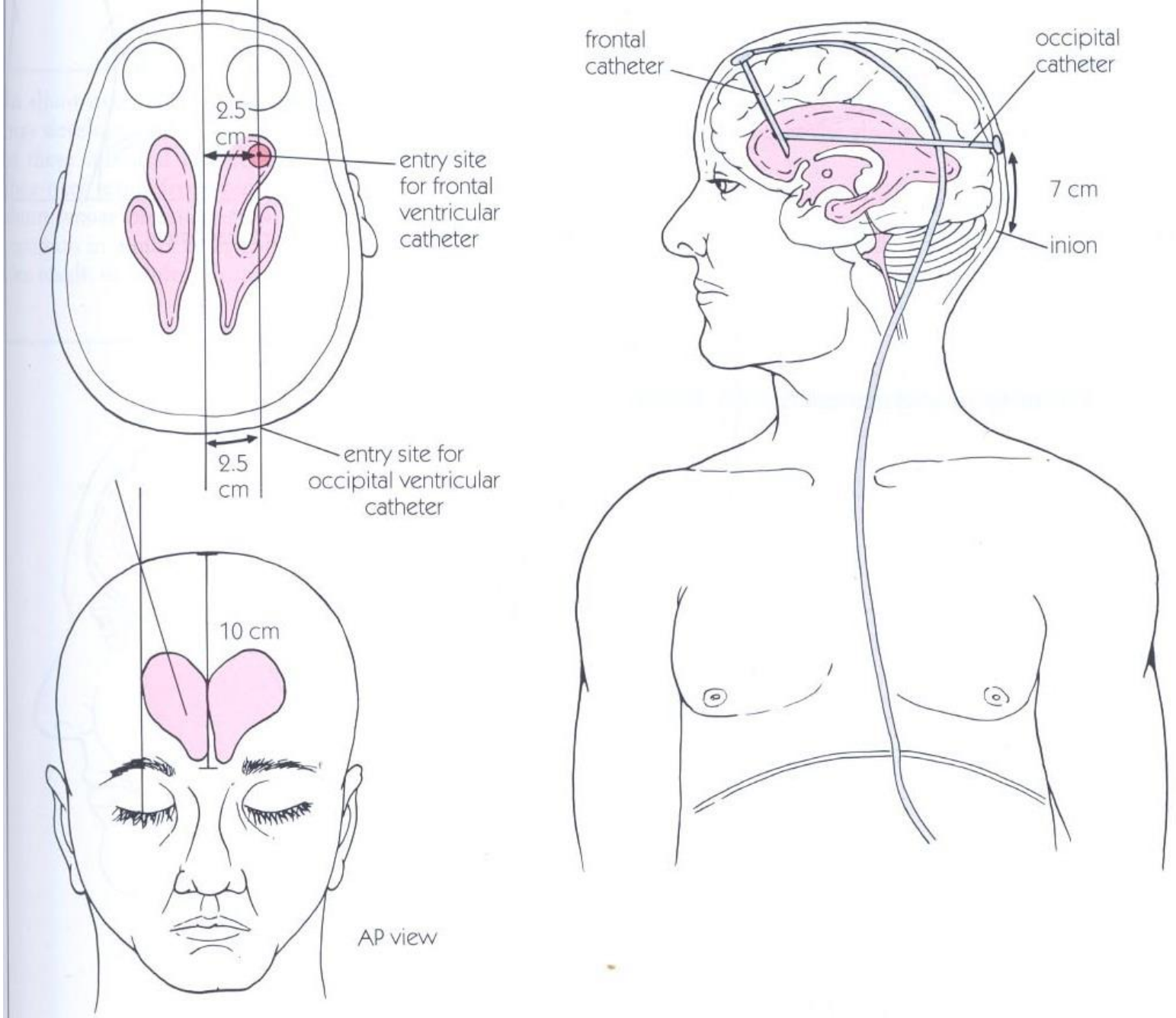

Figure 7.6 Ventriculoperitoneal shunt with a frontal placement. Alternatively, an occipital placement may be used.

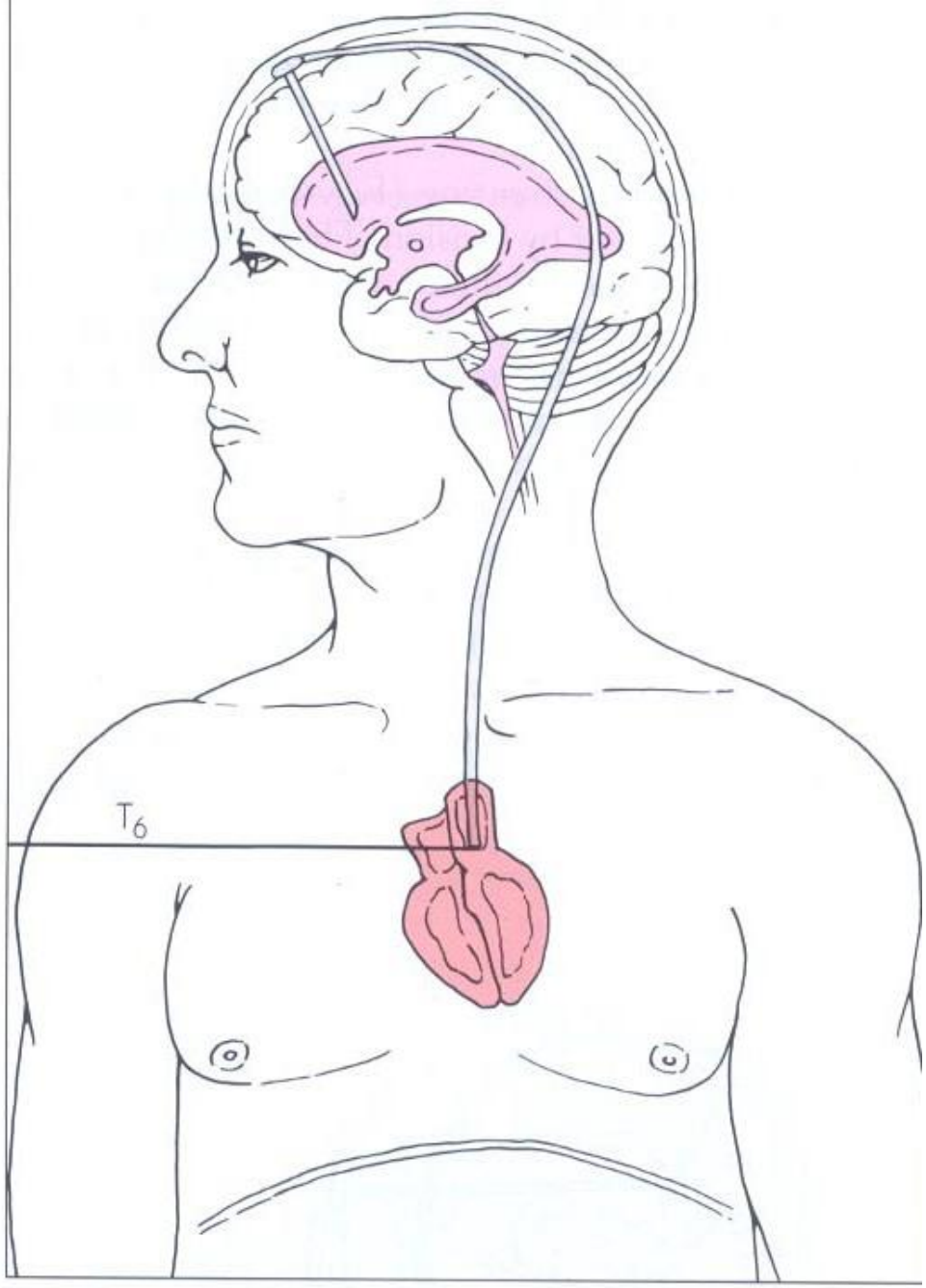

Figure 7.7 Ventriculoatrial shunt placement.

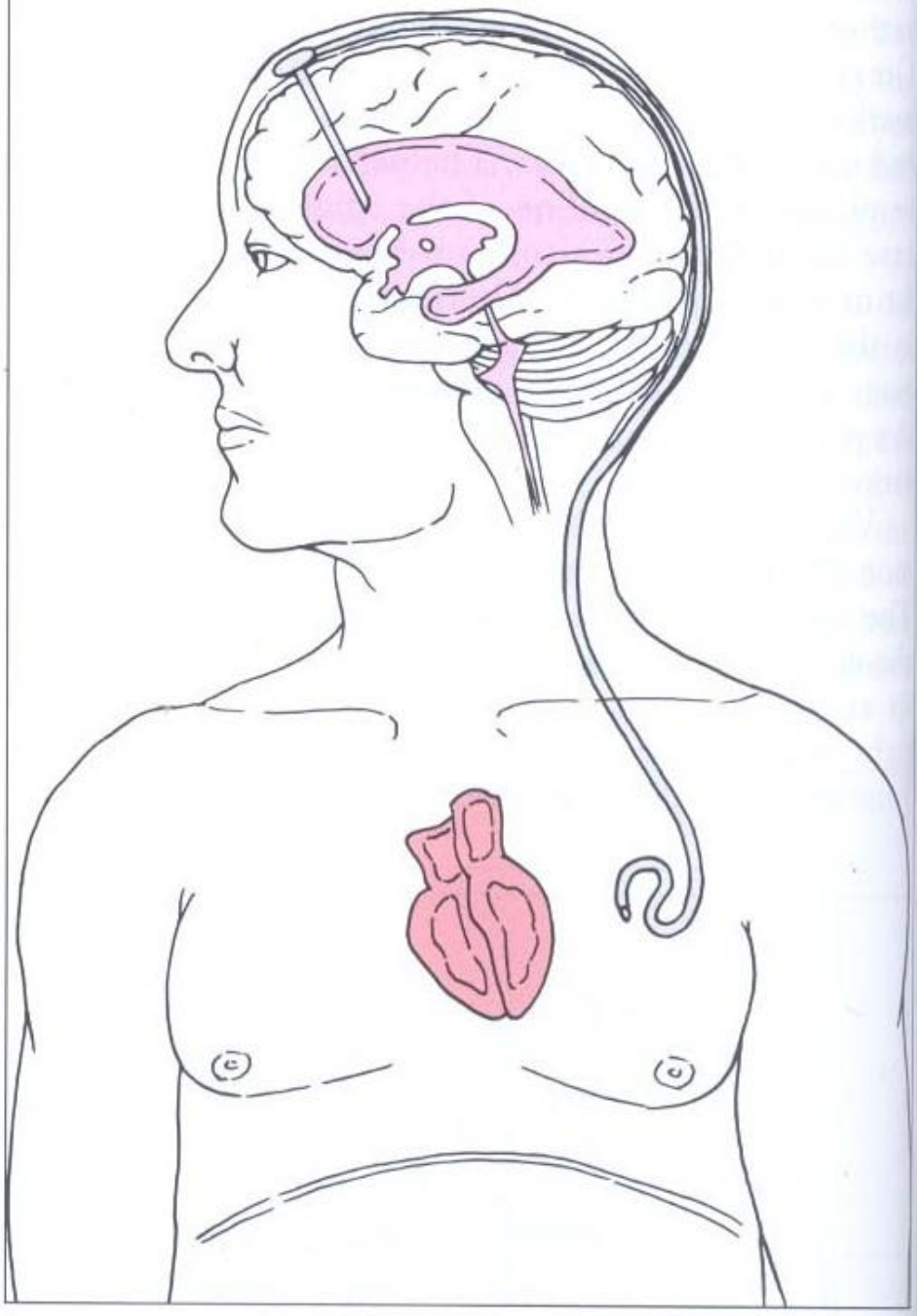

Figure 7.8 Ventriculopleural shunt placement.

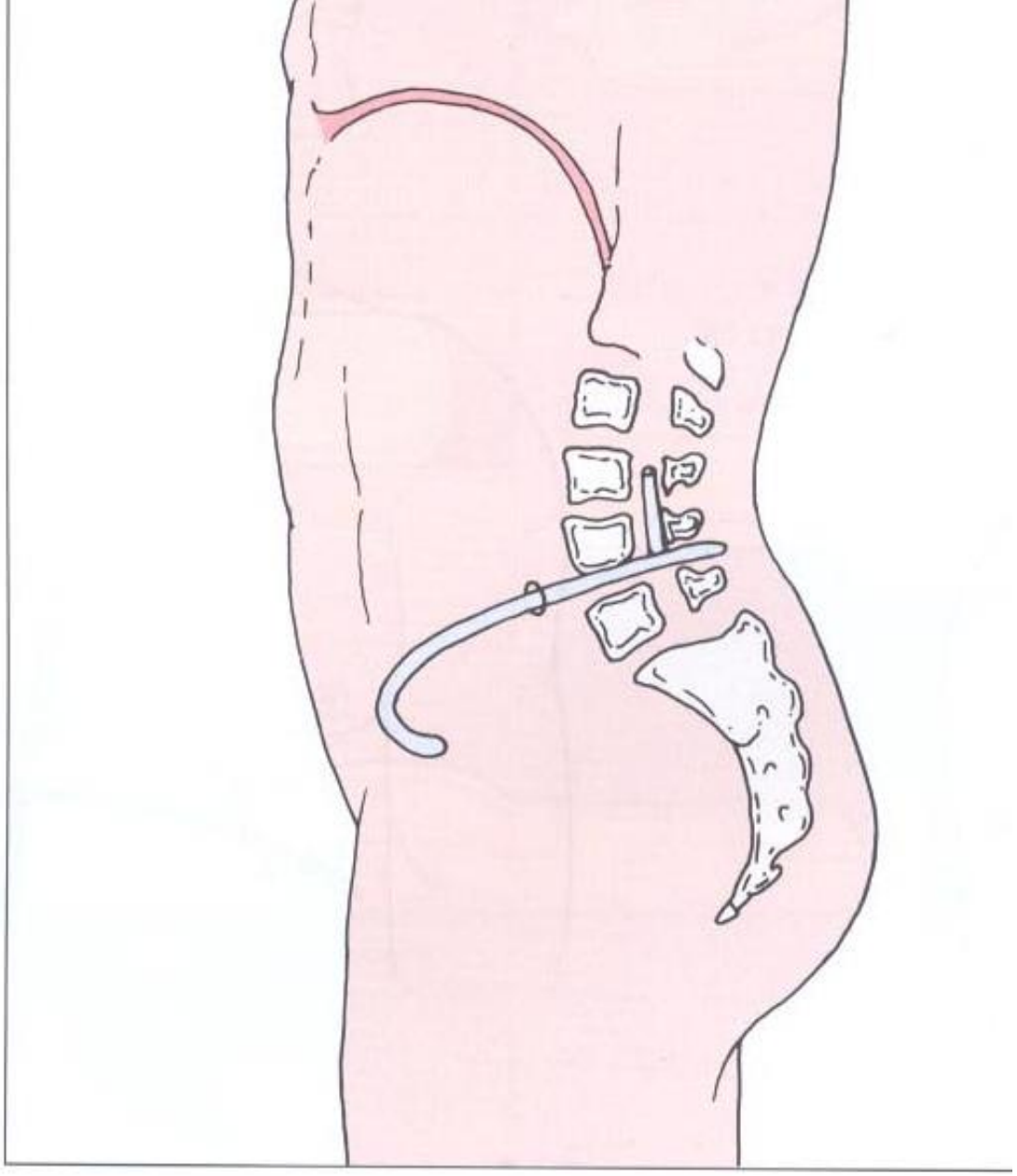

Figure 7.9 Lumboperitoneal shunt placement (for communicating hydrocephalus only).

Ventriculoperitoneal shunting is the easiest and most widely used technique for shunt replacement in adults

Shunt design

Three basic components

- Proximal catheter to access the CSF space
- Valve to regulate the flow
- Distal catheter to drain into the absorptive cavity (usually the peritoneum)

Reservoir

Reservoir is usually included proximal to the valve or as part of the valve construct, allowing percutaneous needle aspiration of CSF for analysis

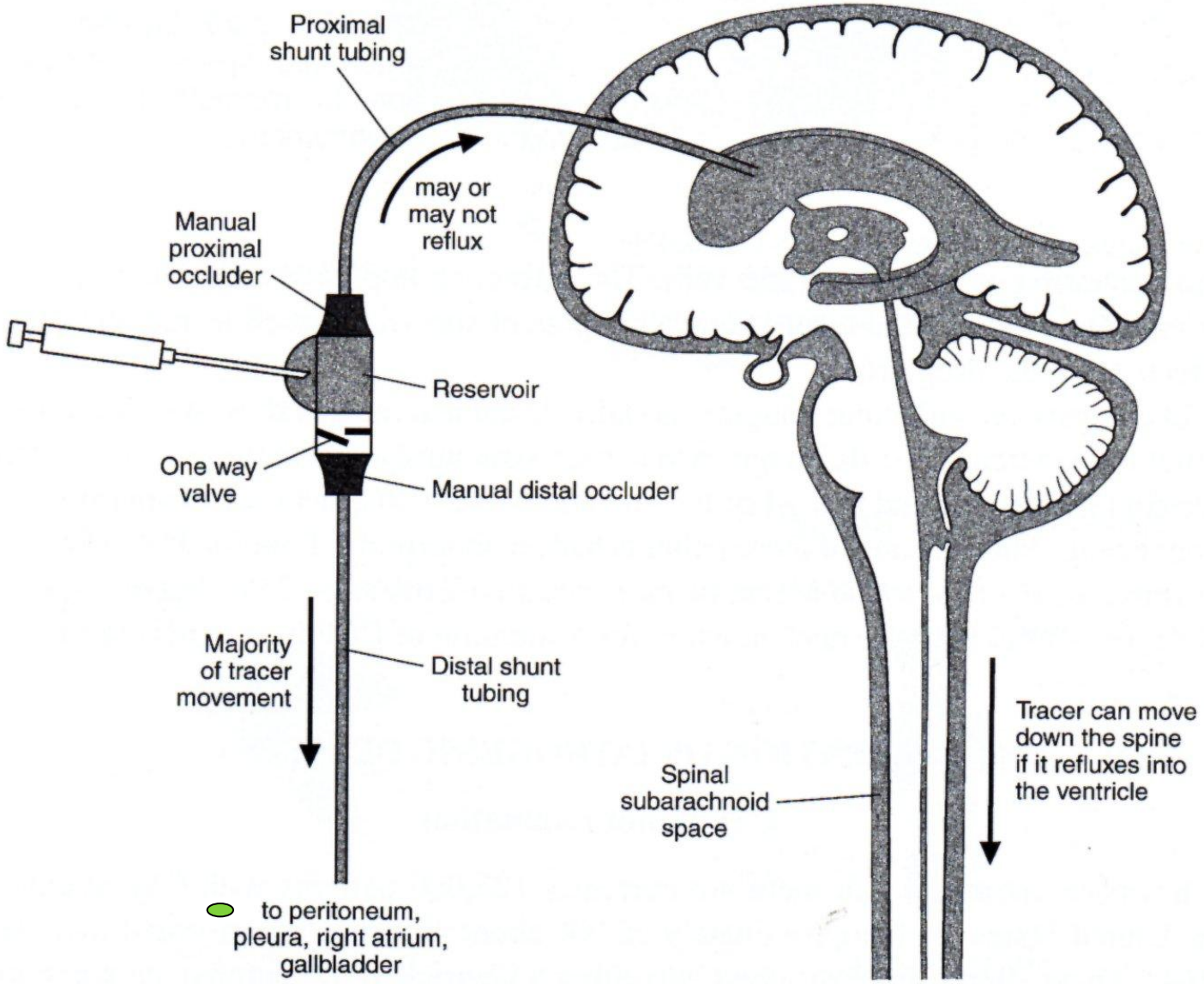

FIGURE 7-30. Diagram of a CSF shunt and the route of tracer movement following injection into the reservoir.

Figure 7.11 Complications of Shunting

Subdural hematoma
Failure of ventricles to shrink
Infection
Shunt obstruction
Overdrainage and slit ventricle syndrome
Disconnection of shunt components
Perforation of hollow viscus by the peritoneal catheter

Radionuclide Shuntogram

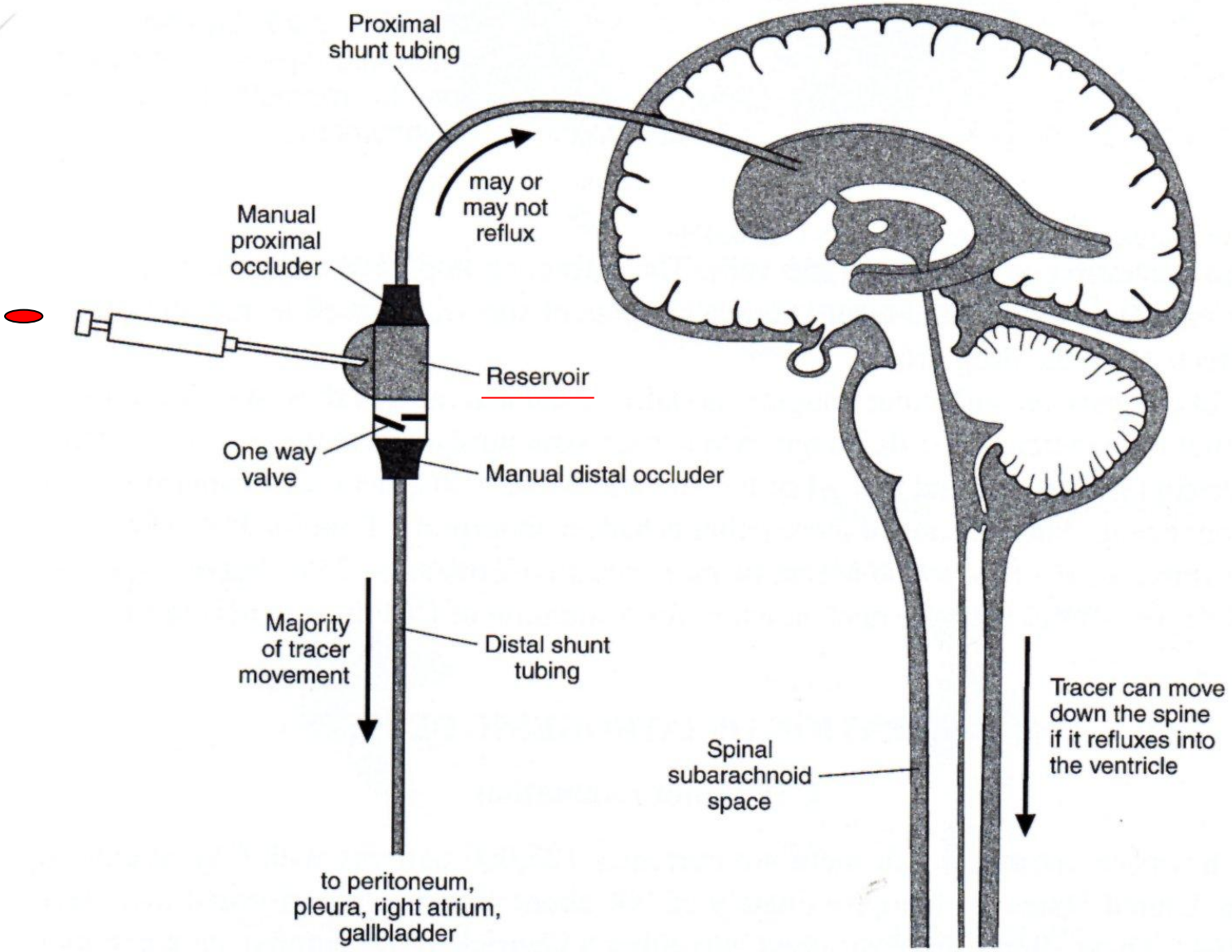

FIGURE 7-30. Diagram of a CSF shunt and the route of tracer movement following injection into the reservoir.

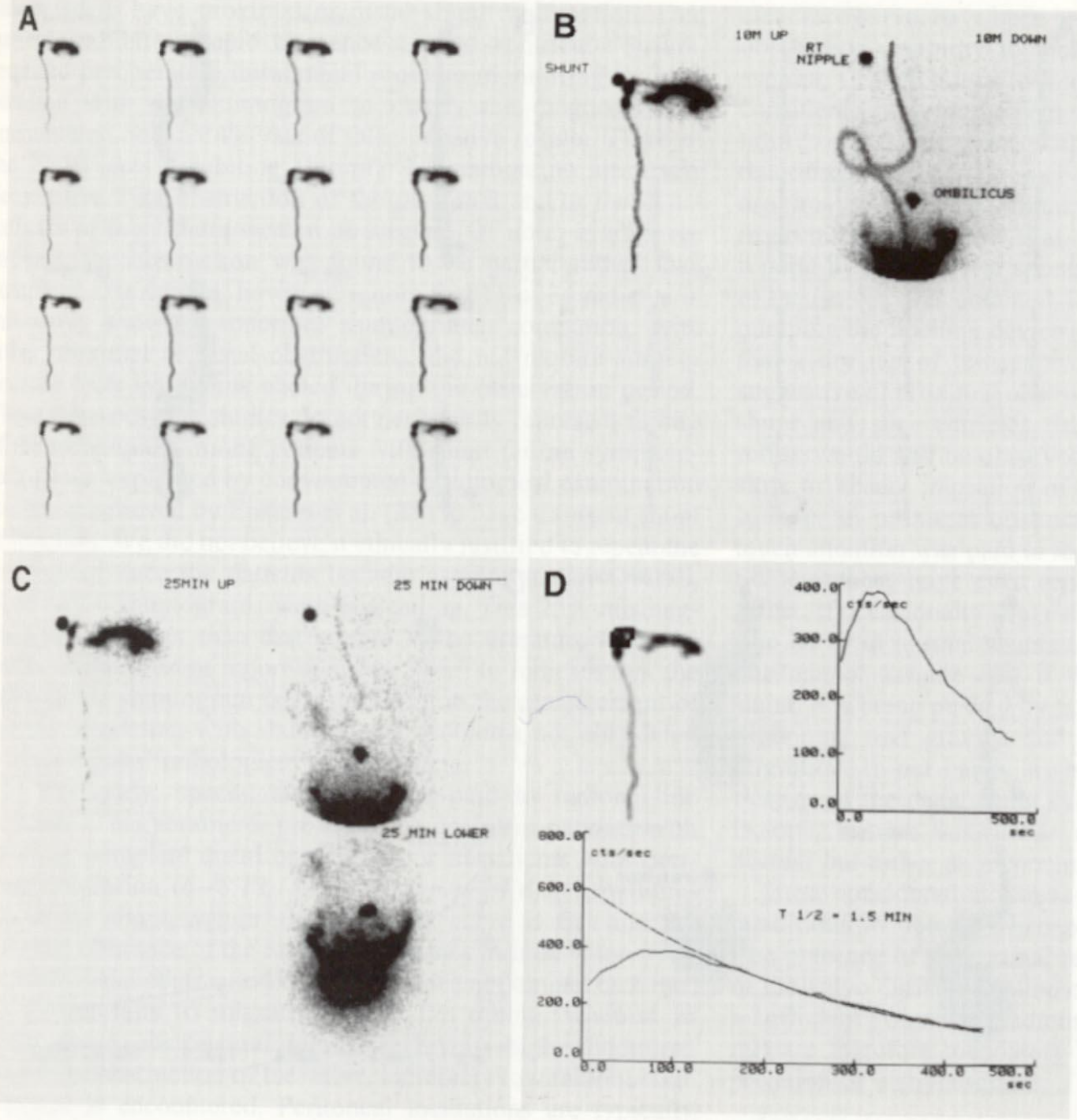

FIGURE 1. Normal shuntogram. (A Immediate postinjection sequenc (1 frame/15 sec) shows ventricular reflu and some migration of activity into th distal tubing. (B,C) Static views of th head and abdomen demonstrate ir creasing activity in the abdomen. (D Time-activity curve of the reservoir (y = cps, x = sec).

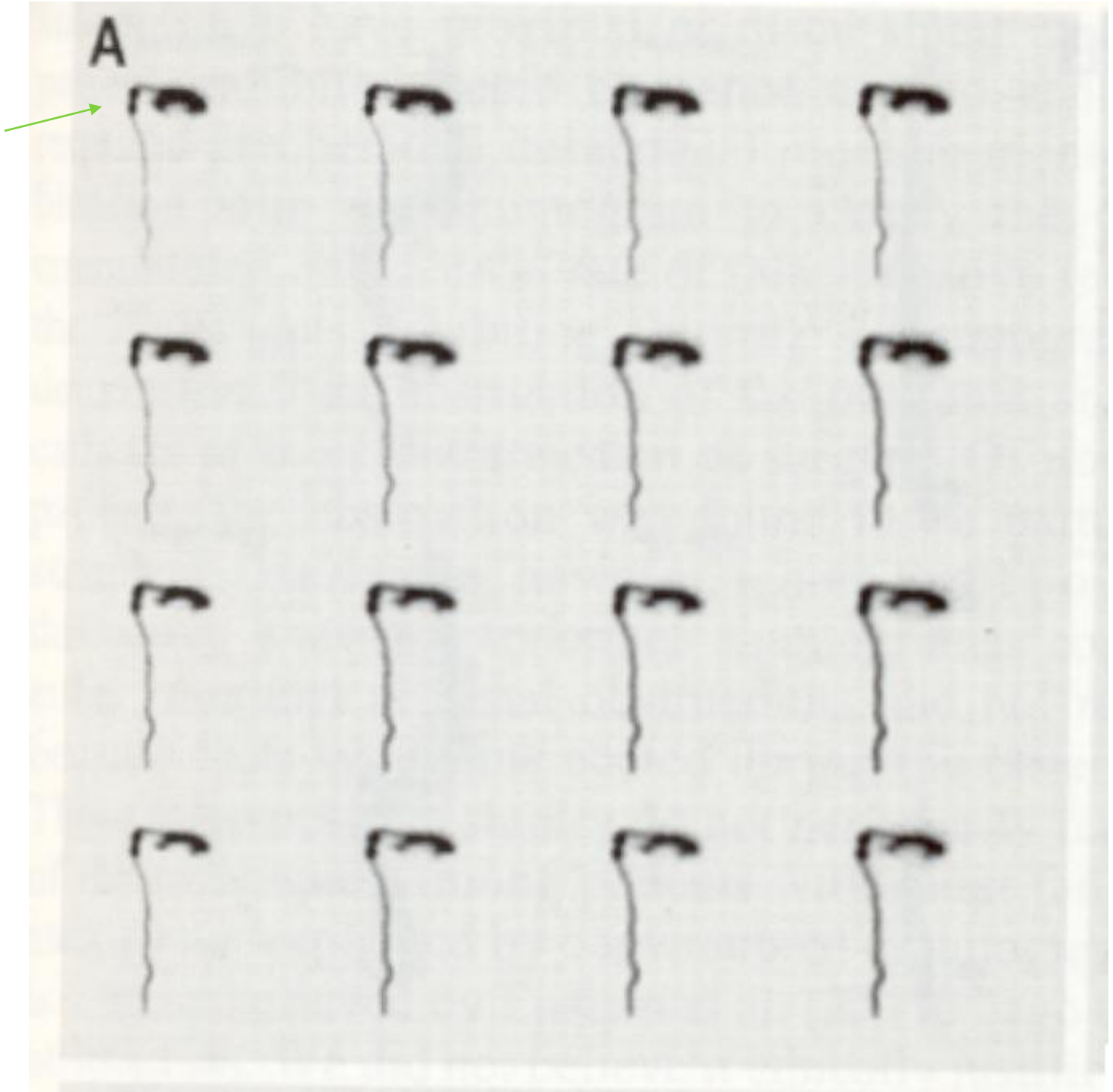
A

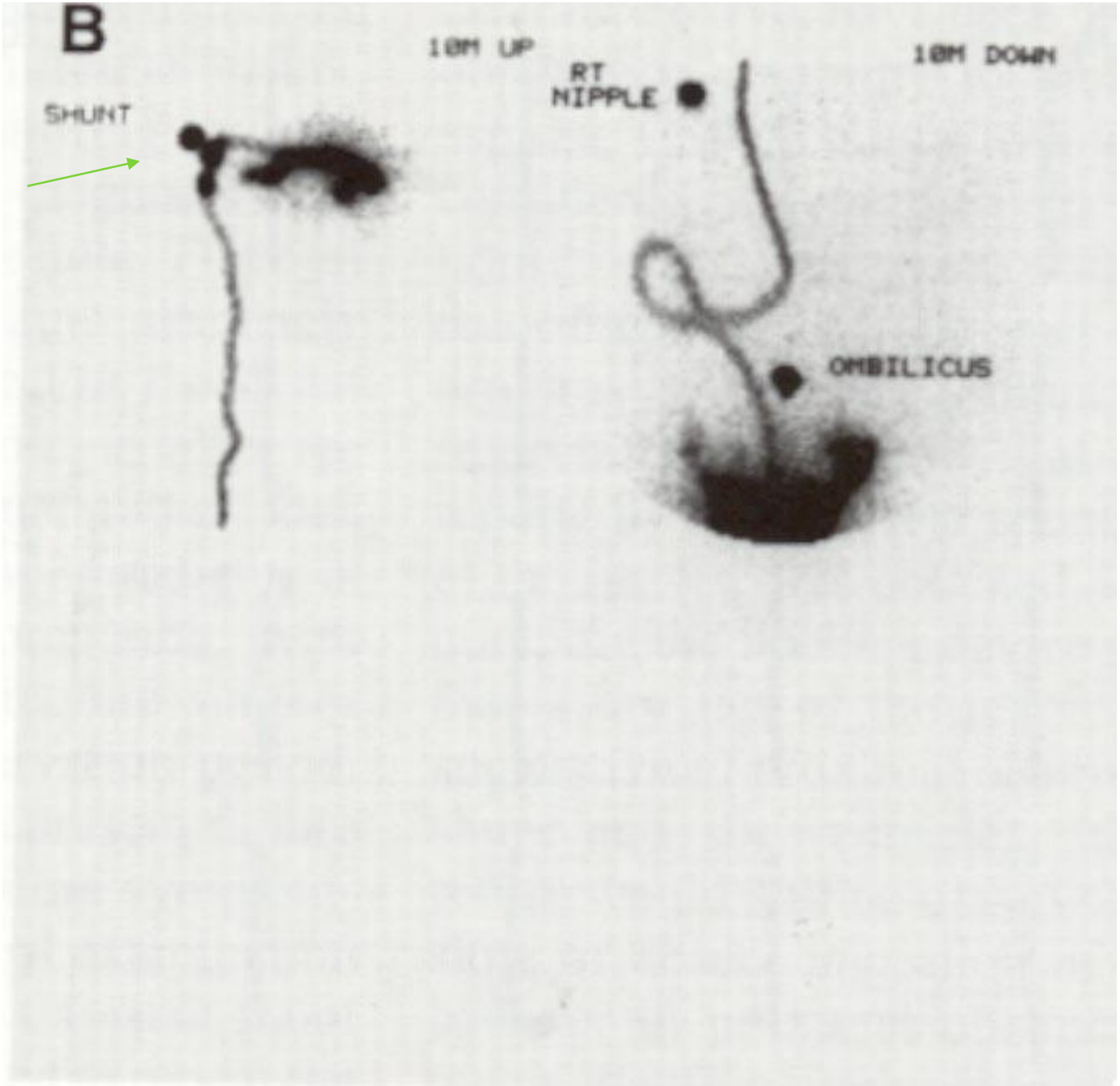
B
10M UP
10M DOWN
SHUNT
RT
NIPPLE
OMBILICUS

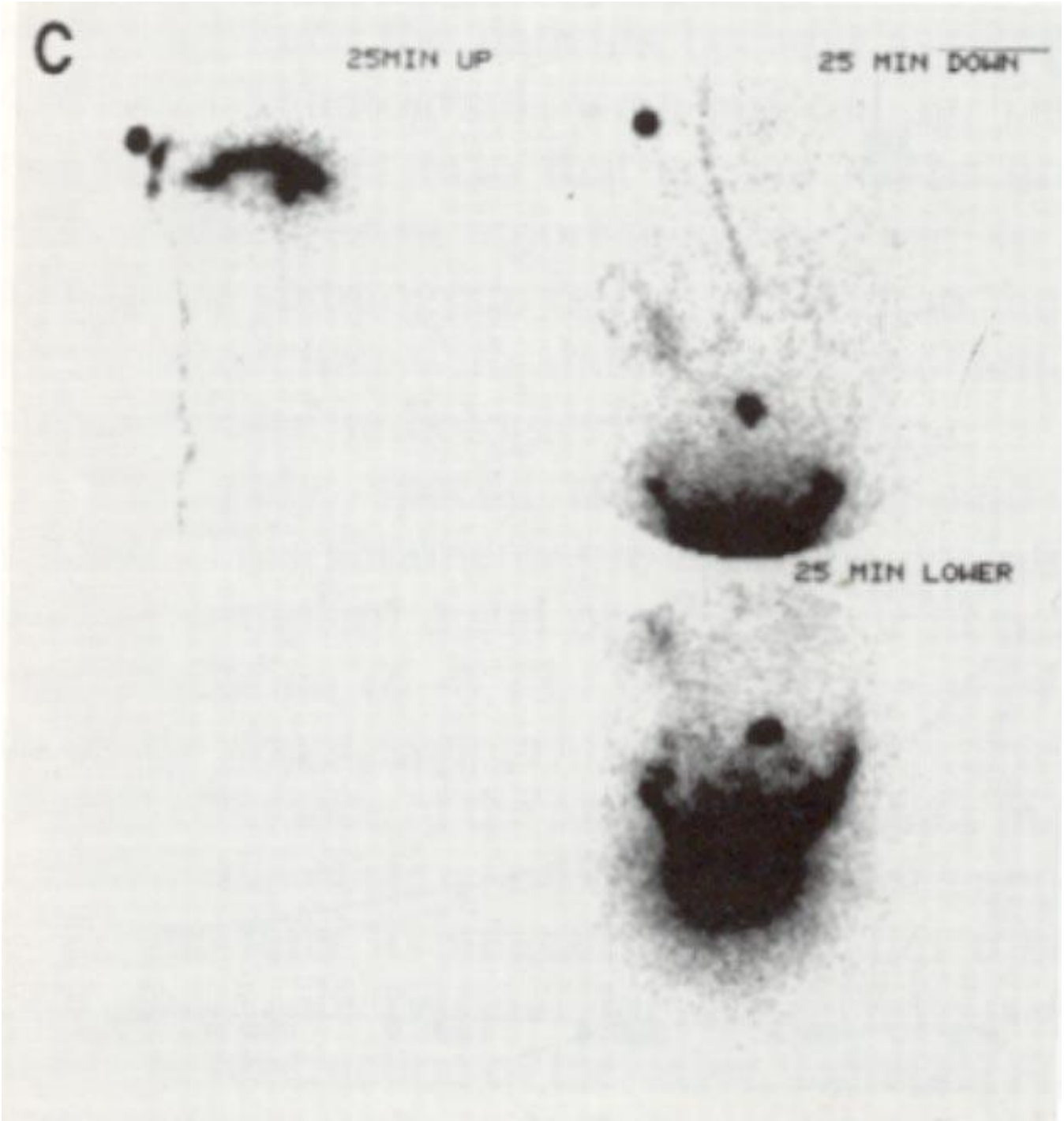
C
25MIN UP
25 MIN DOWN
25 MIN LOWER

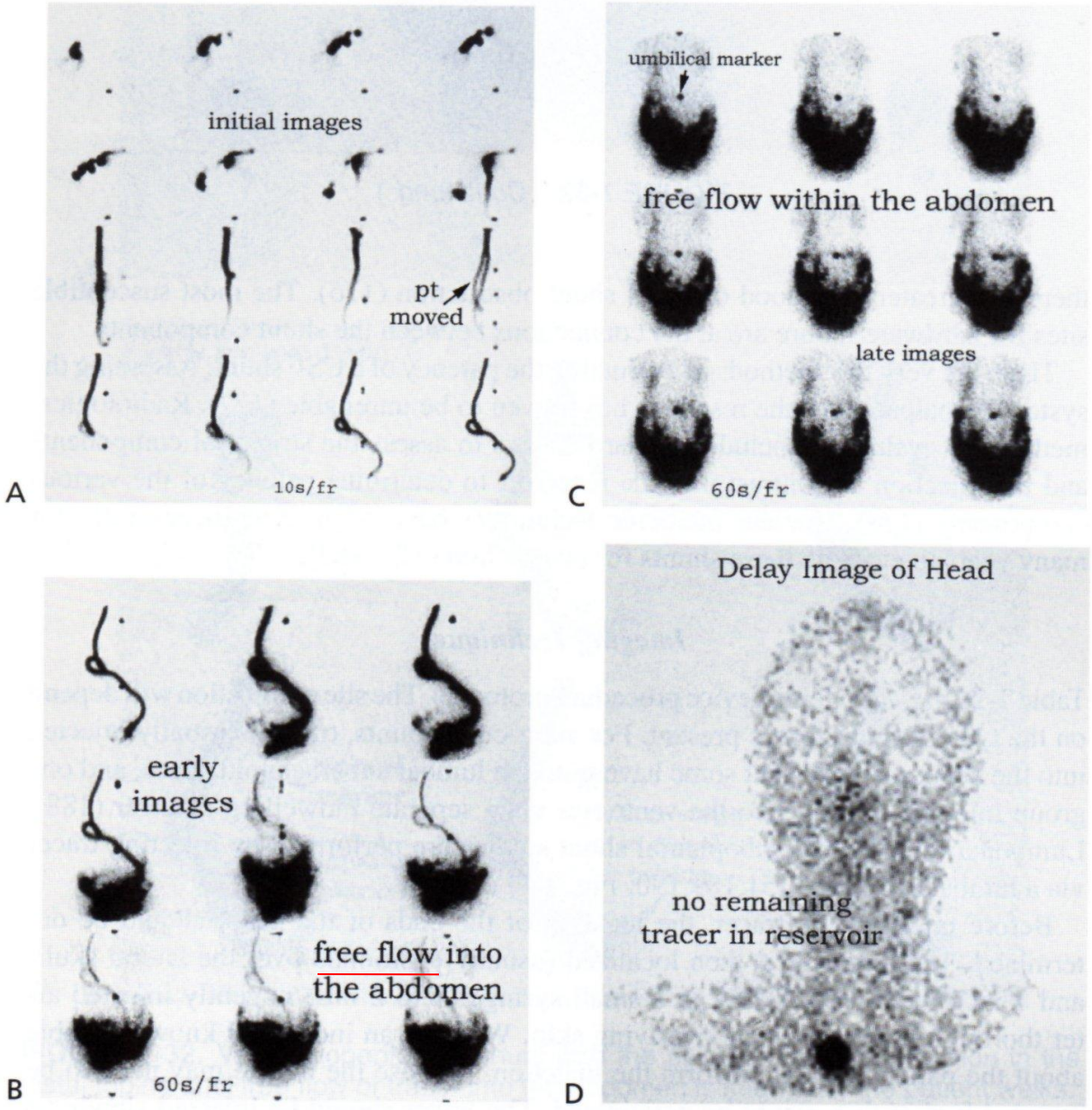

FIGURE 7-33. Patent ventriculoperitoneal shunt; no residual activity is seen in the shunt reservoir on a delayed cerebral image.

Table 57.2 CSF shunt tracer patterns

Normal
Ventricular reflux
Rapid transit into blood (VA), peritoneum (VP), pleural cavity (VPI)
Transit time <45 min
Rapid transit from lumbar SAS to peritoneum (LP)
Abnormal CSF flow patterns
No flow (Fig. 57.10)
No ventricular reflux
Breaks in column and patent distal end (proximal block)
No peritoneal or blood pool activity (distal block) (Fig. 57.11)
Flow for lumbar SAS to basal cisterns (block LP)
Extravasation at connector of reservoir or valve
Extravasation or tracking along shunt pathway
Loculation at distal end (Fig. 57.12)

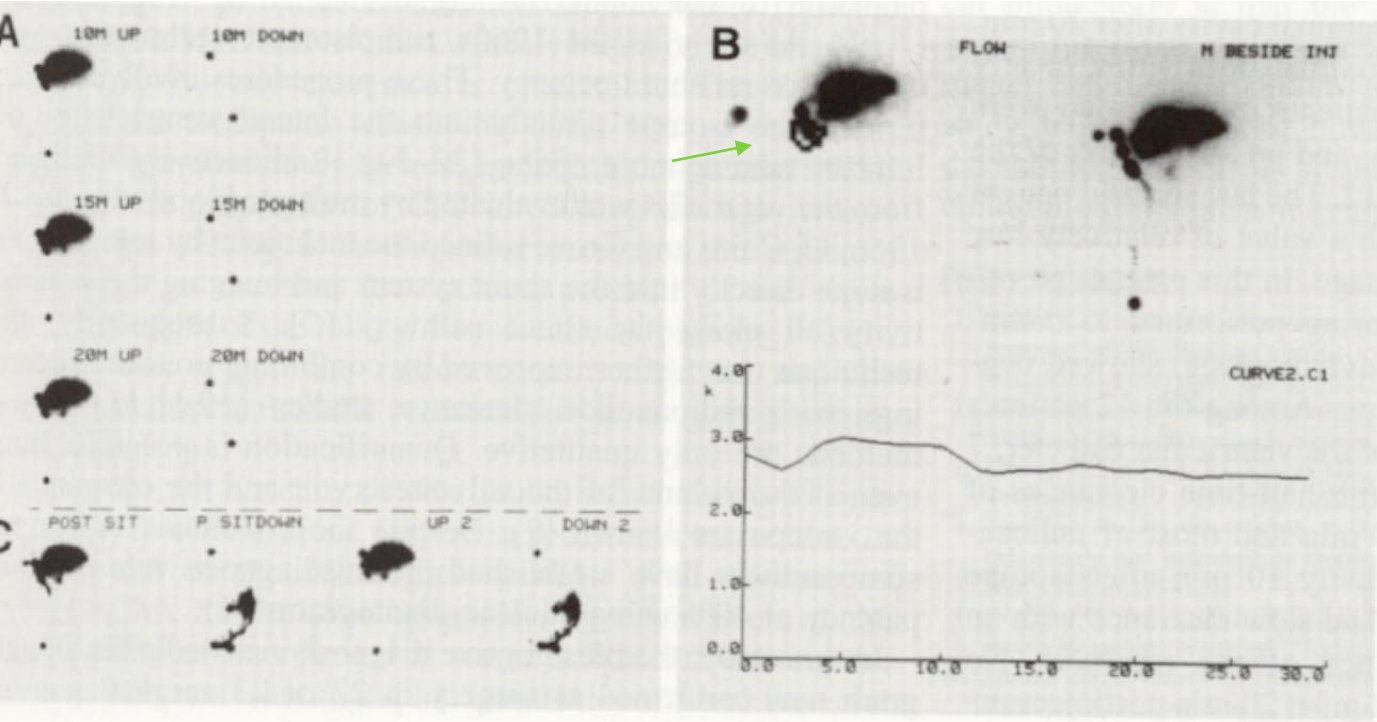

FIGURE 2. Shuntogram with distal ob
struction. (A) Static views at 10, 15, 2
min show ventricular reflux but no migra
tion of radioactivity in the distal tubing. (E
Shunt reservoir's time-activity curve is fla
with no washout (y = kcps, x = min). (C
After imaging in the sitting position an
pumping the valve, there is some radio
activity in a peritoneal loculation.

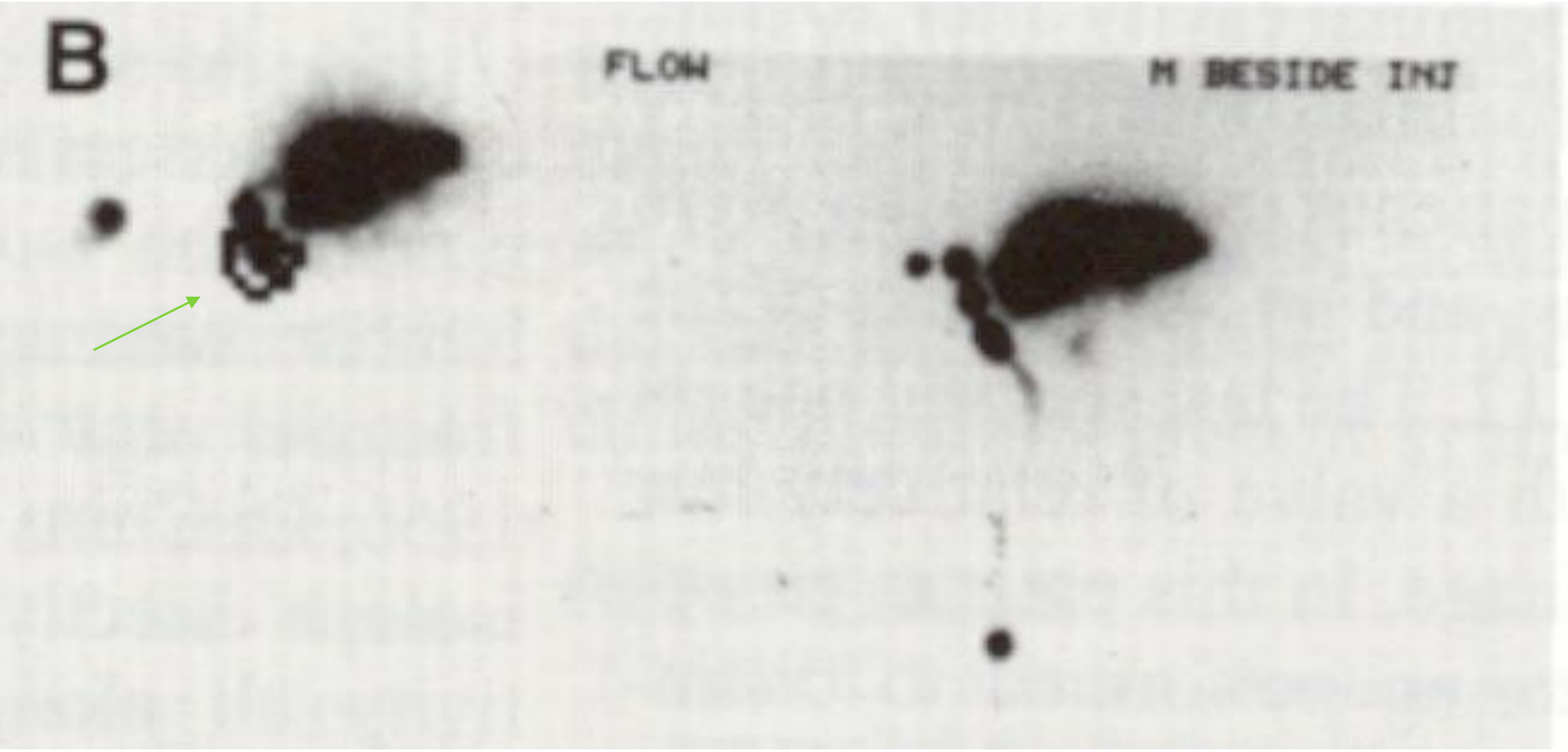
B
FLOW
M BESIDE INJ

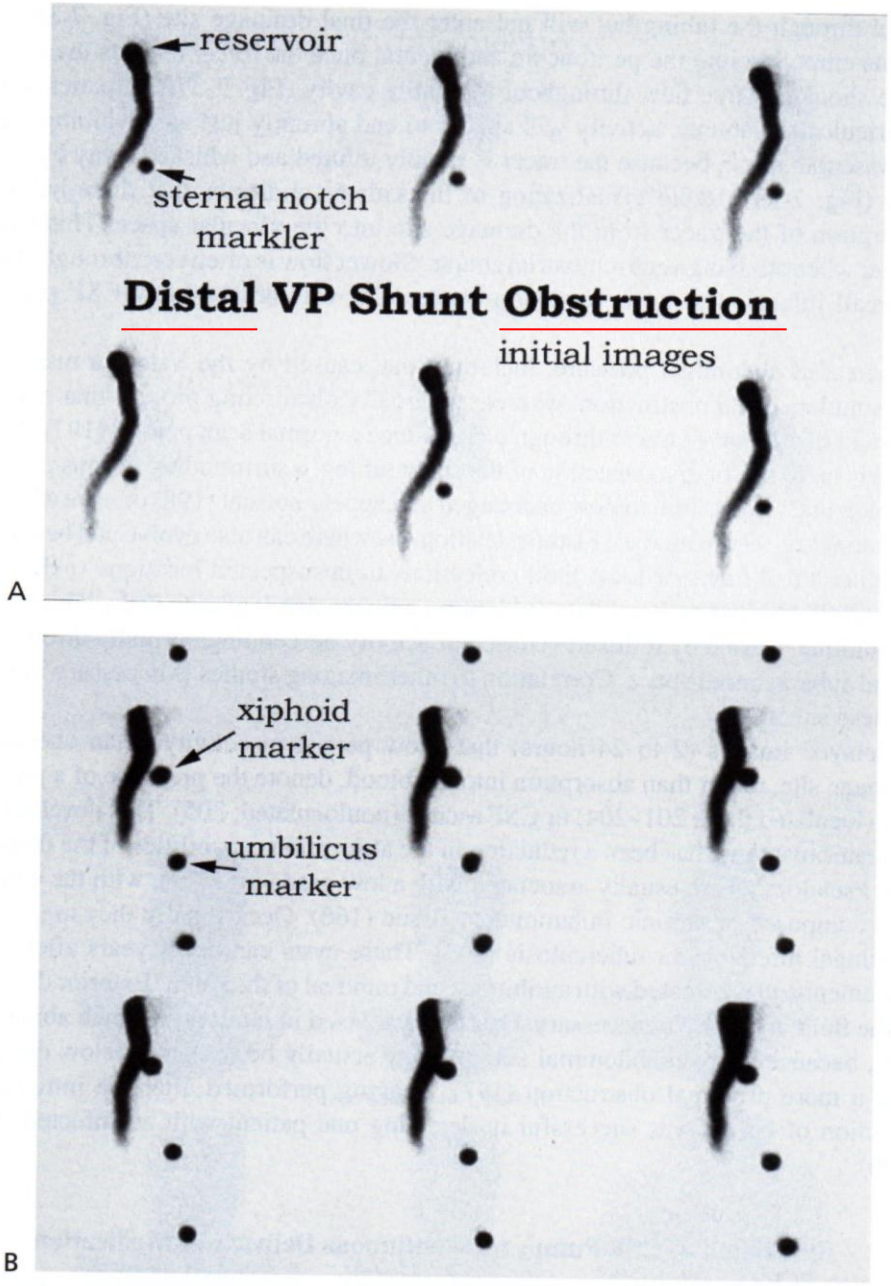

FIGURE 7-36. Distal ventriculoperitoneal shunt obstruction; tracer moves through the tubing with walking and shunt pumping, but does not empty into the abdomen.

Detection of Gastrointestinal Bleeding

Tc-99m red blood cell scintigraphy

Box 11-9 Methods of Technetium-99m Red Blood Cell Labeling

IN VIVO METHOD

(labeling efficiency, 75% to 80%)

1. Inject stannous pyrophosphate.
2. Wait 10 to 20 min.
3. Inject Tc-99m sodium pertechnetate.

MODIFIED IN VIVO (IN VITRO) METHOD

(labeling efficiency, 85% to 90%)

1. Inject stannous pyrophosphate.
2. Wait 10 to 20 min.
3. Withdraw 5 to 8 ml of blood into shielded syringe with technetium-99m.
4. Gently mix syringe contents for 10 min at room temperature.

IN VITRO (BROOKHAVEN) METHOD

(labeling efficiency, 98%)

1. Add 4 ml of heparinized blood to reagent vial of 2 mg Sn^{+2}, 3.67 mg Na citrate, 5.5 mg dextrose, and 0.11 mg NaCl.
2. Incubate at room temperature for 5 min.
3. Add 2 ml of 4.4% EDTA.
4. Centrifuge tube for 5 min at 1300 *g*.
5. Withdraw 1.25 ml of packed RBCs and transfer to sterile vial containing 1 to 3 ml of Tc-99m.
6. Incubate at room temperature for 10 min.

IN VITRO COMMERCIAL KIT

(labeling efficiency, 98%)

1. Add 1 to 3 ml of blood (heparin or acid citrate dextrose as anticoagulant) to reagent vial (50 to 100 µg stannous chloride, 3.67 mg Na citrate) and mix. Allow 5 min to react.
2. Add syringe 1 contents (0.6 mg sodium hypochlorite) and mix by inverting four or five times.
3. Add contents of syringe 2 (8.7 mg citric acid, 32.5 mg Na citrate, dextrose) and mix.
4. Add 370 to 3700 MBq (10 to 100 mCi) of Tc-99m to reaction vial.
5. Mix and allow to react for 20 min, with occasional mixing.

Box 11-11 Criteria for Positive Technetium-99m Red Blood Cell Scintigraphy

"Hot spot" appears and conforms to intestinal anatomy.
Abnormal activity increases over time.
Abnormal activity moves antegrade or retrograde through bowel (essential criterion).

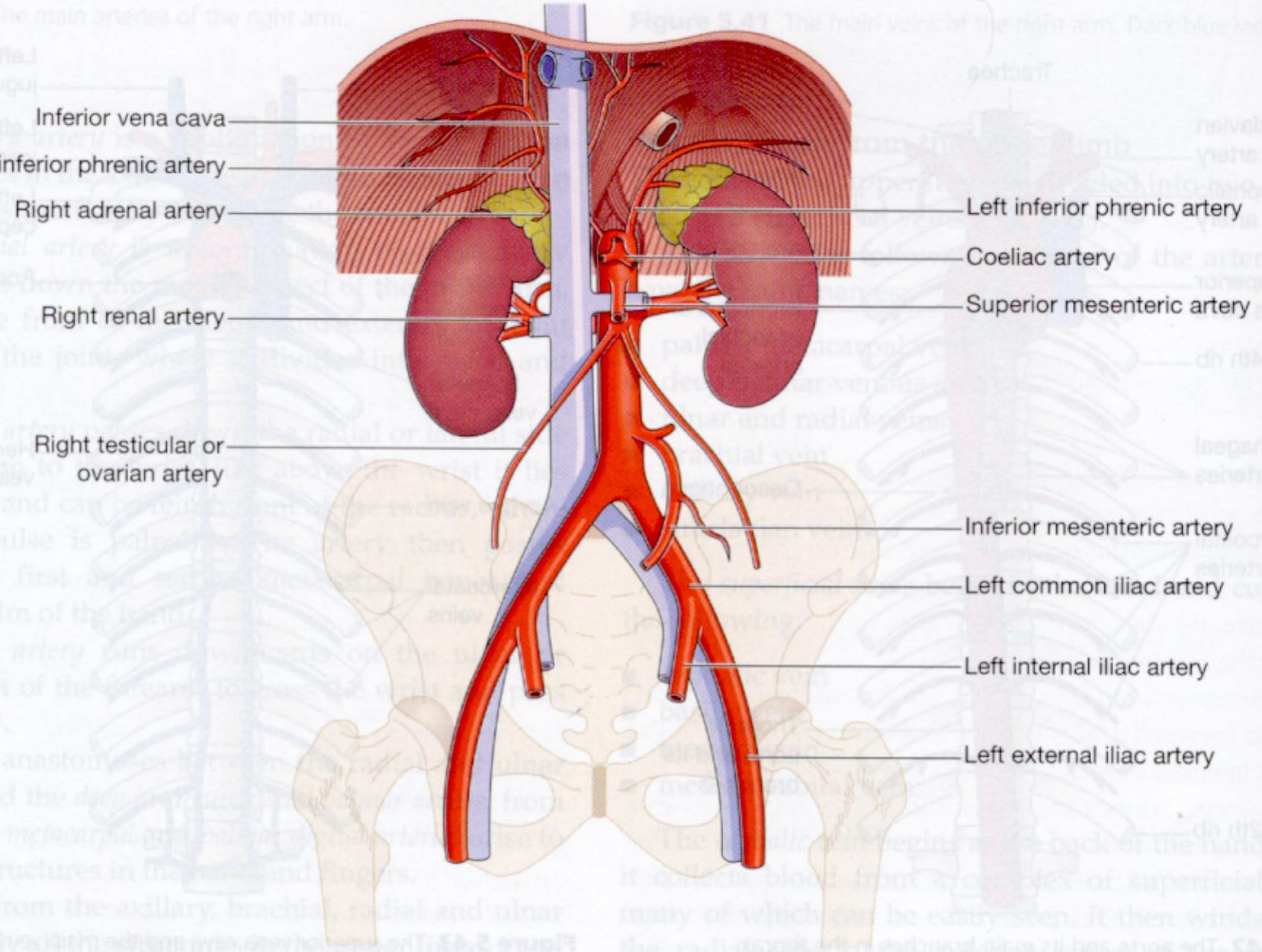

Figure 5.44 The abdominal aorta and its branches.

Normal gastrointestinal tract bleeding study

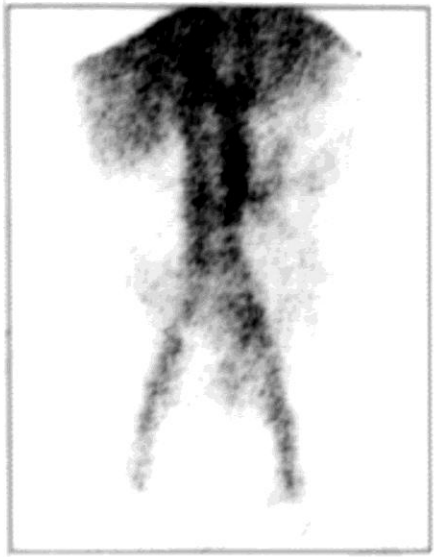

a 2 minutes

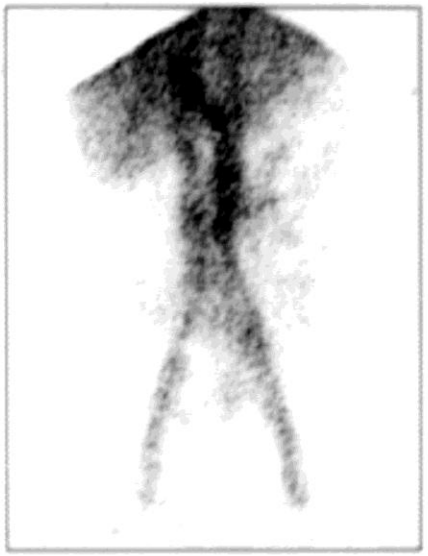

b 10 minutes

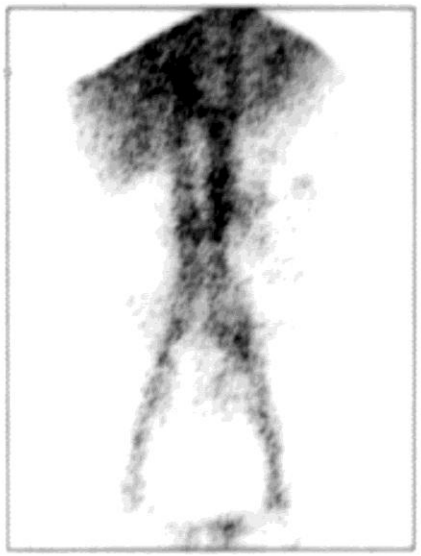

c 20 minutes

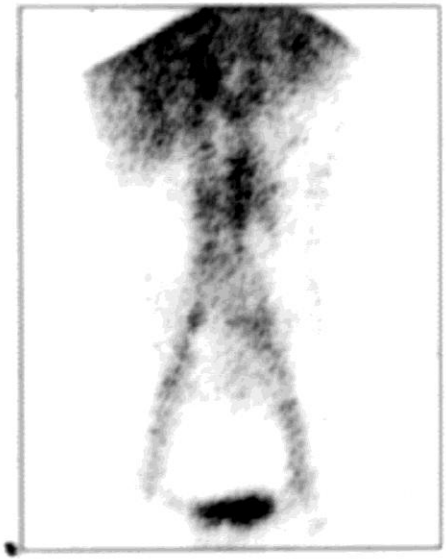

d 35 minutes

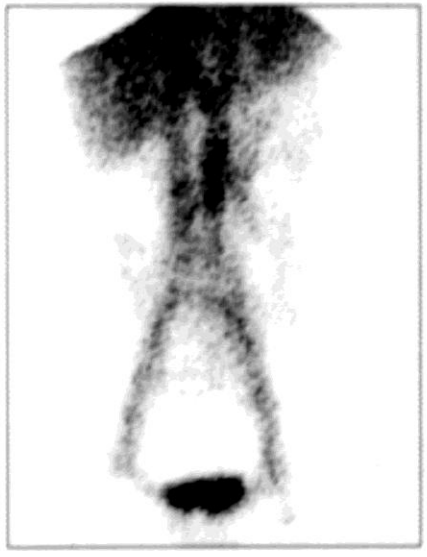

e 45 minutes

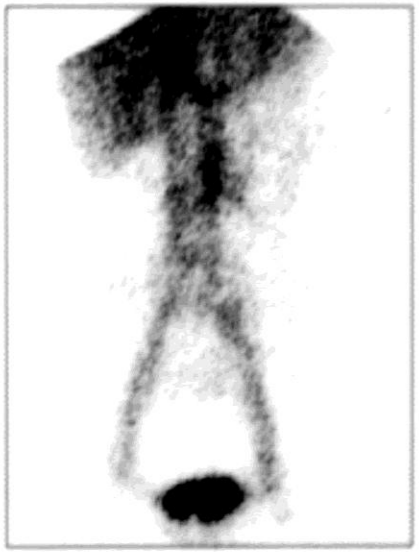

f 50 minutes

Fig. 9.60

(a–f) *^{99m}Tc RBC study.*

This is a normal study with no evidence of any active gastrointestinal bleeding. Although it is a good quality study, note that, with time, there is increasing tracer activity in the bladder caused by free pertechnetate.

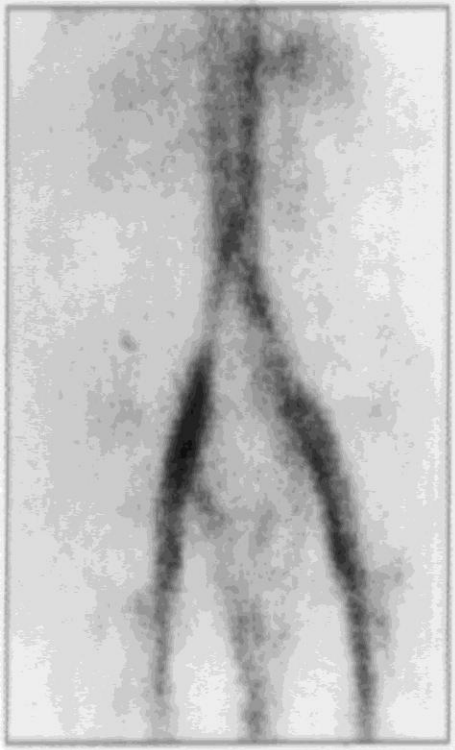

a 2 minutes

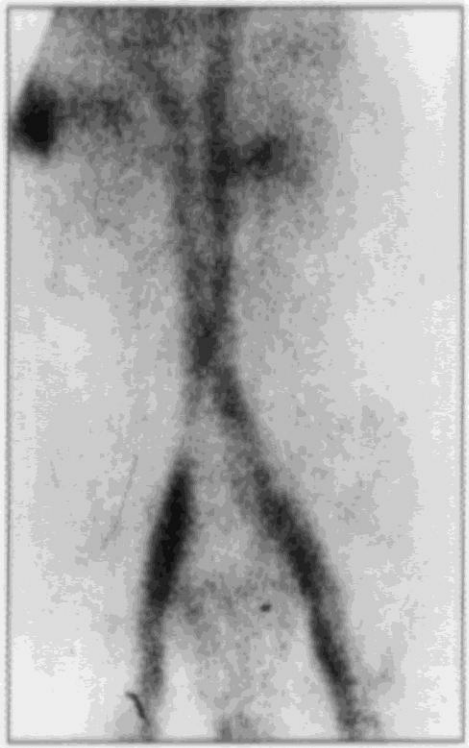

b 15 minutes

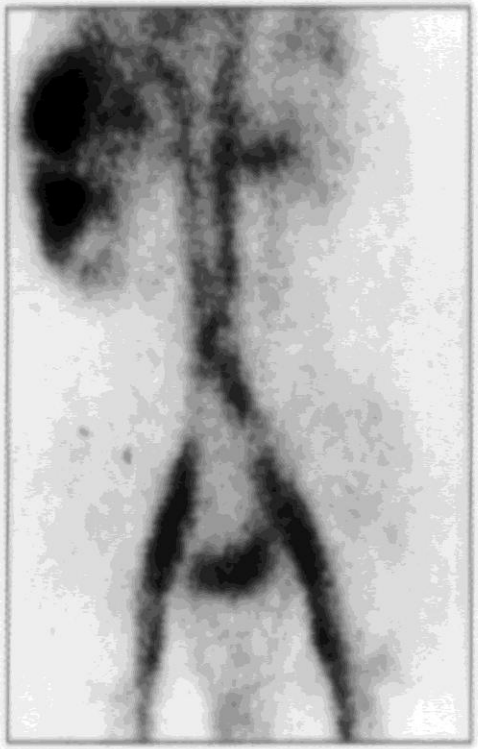

c 25 minutes

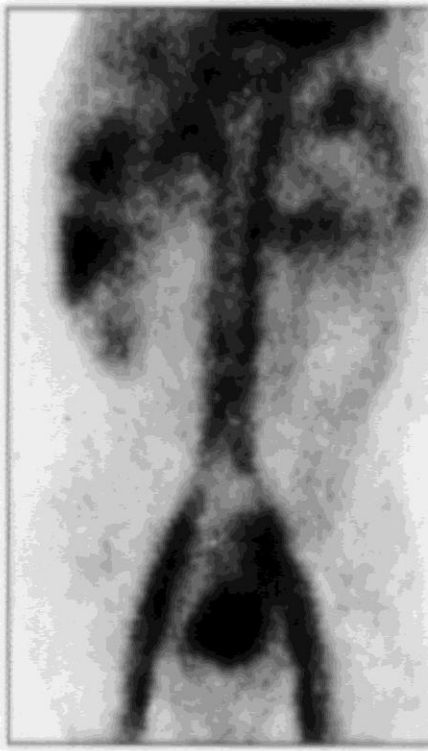

d 35 minutes

Fig. 9.63

(a–d) ^{99m}Tc RBC study.

The patient was a 64-year-old man with gastrointestinal bleeding. There is tracer accumulation visualized in the right upper quadrant of the abdomen. Activity is clearly visualized by 15 minutes, and there is subsequent accumulation and passage across the abdomen. This is a positive study which indicates active bleeding, the site of origin being most likely in the upper ascending colon.

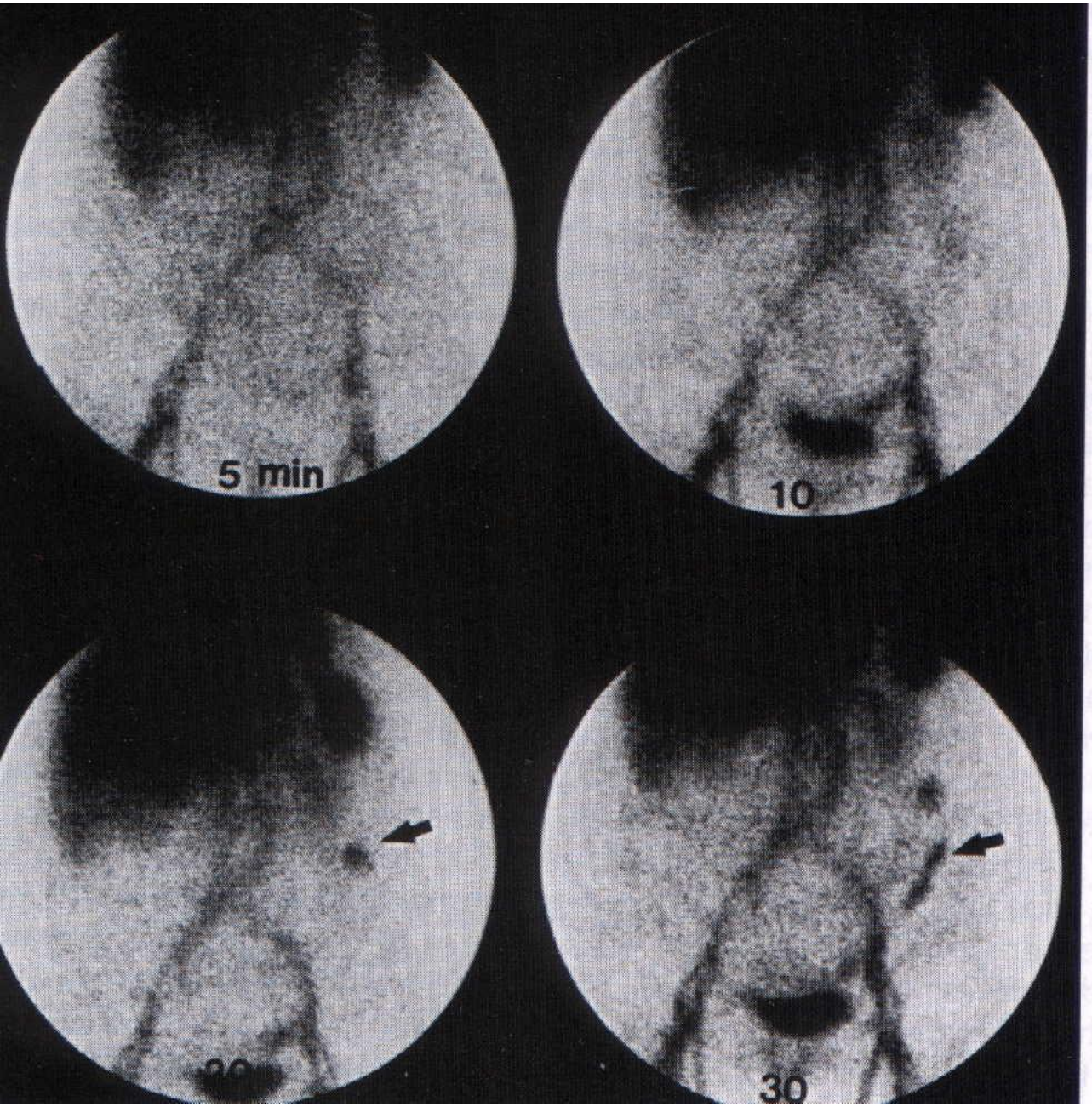

Figure 10-20. Gastrointestinal bleeding. This study was performed with ^{99m}Tc labeled red blood cells and at 20 minutes demonstrates a focus of active bleeding in the descending colon *(arrow)*, which on the later views can be seen in the bowel distally.

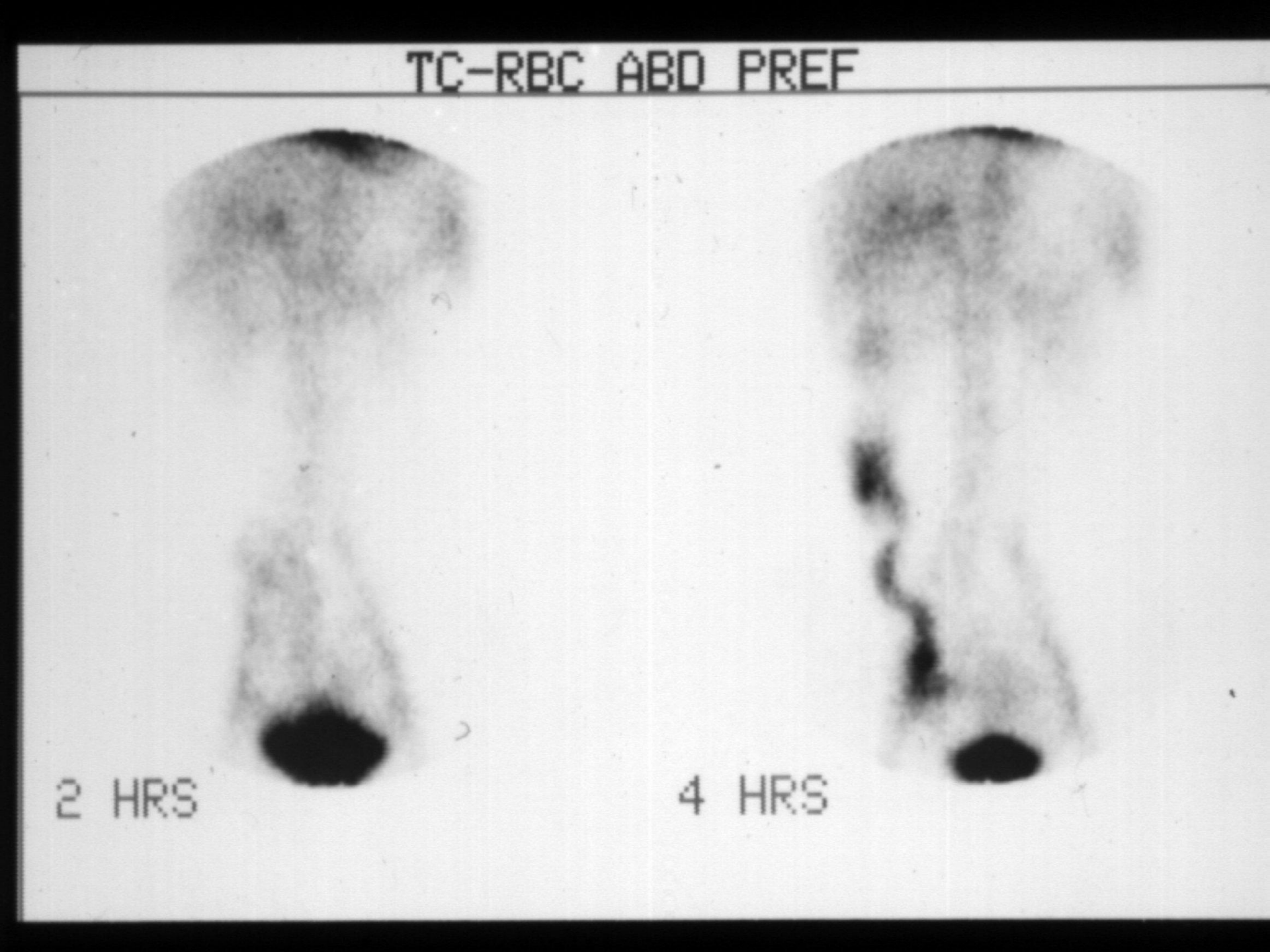
TC-RBC ABD PREF
2 HRS
4 HRS

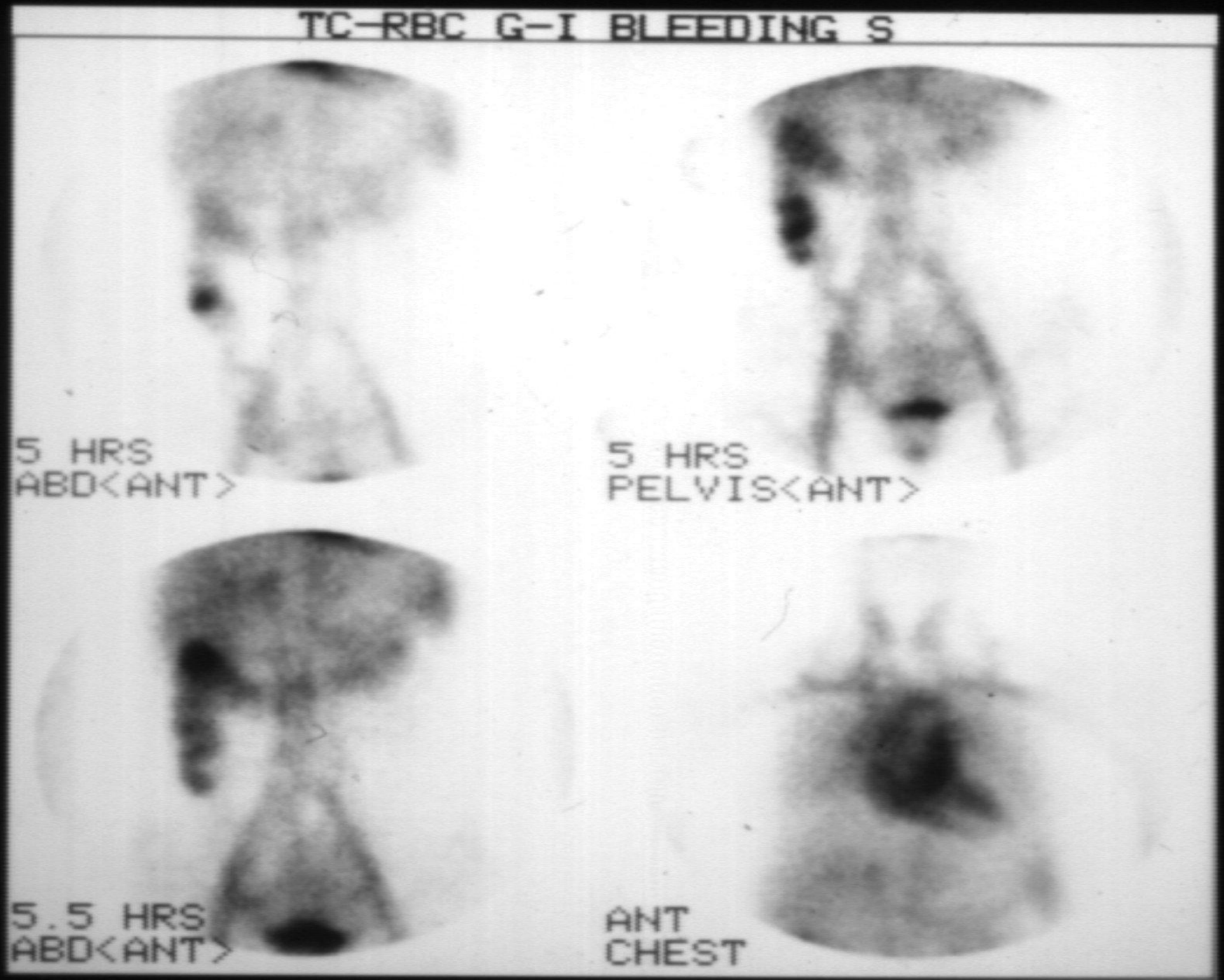
TC-RBC G-I BLEEDING S
5 HRS
ABD<ANT>
5 HRS
PELVIS<ANT>
5.5 HRS
ABD<ANT>
ANT
CHEST

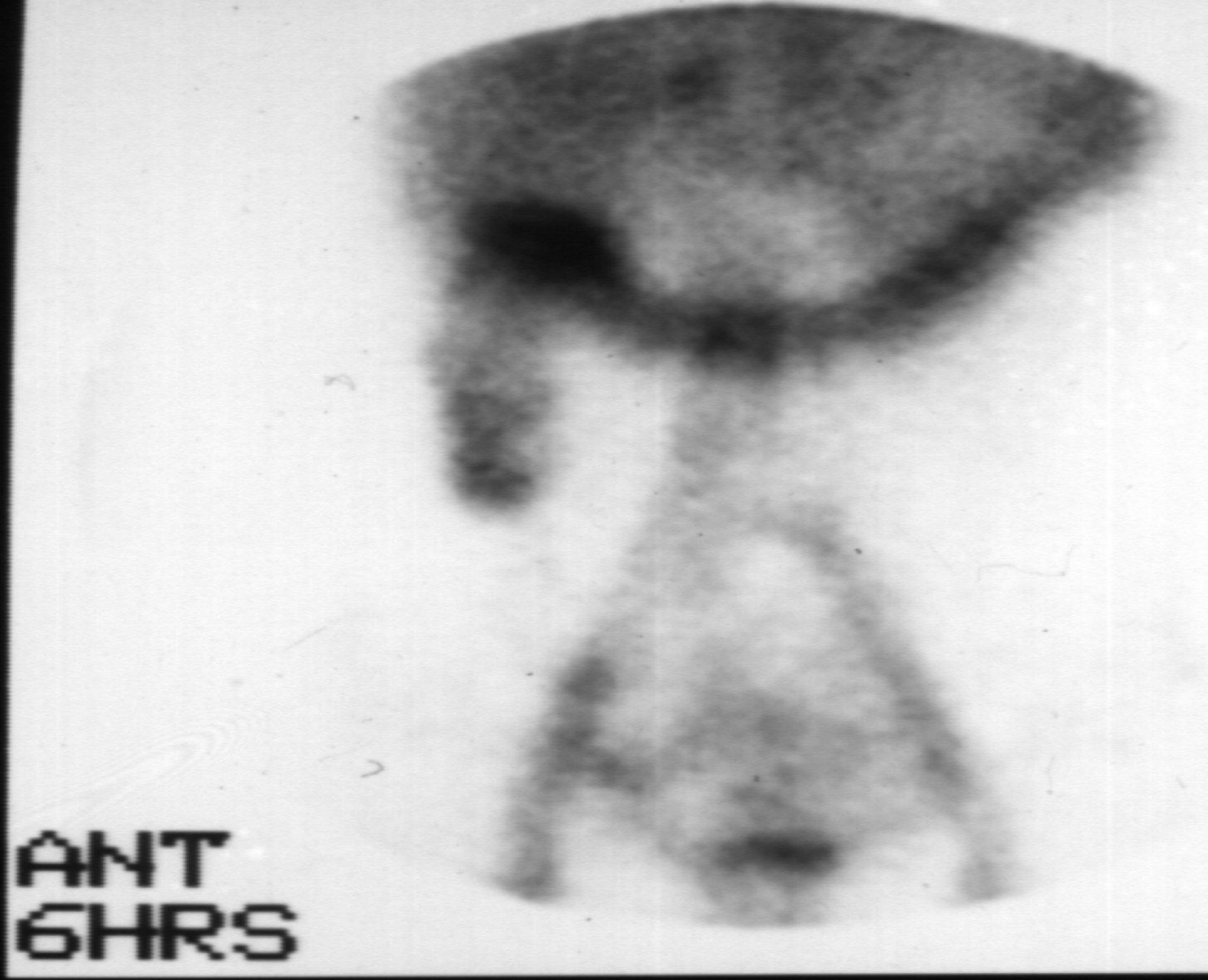
ANT
6HRS

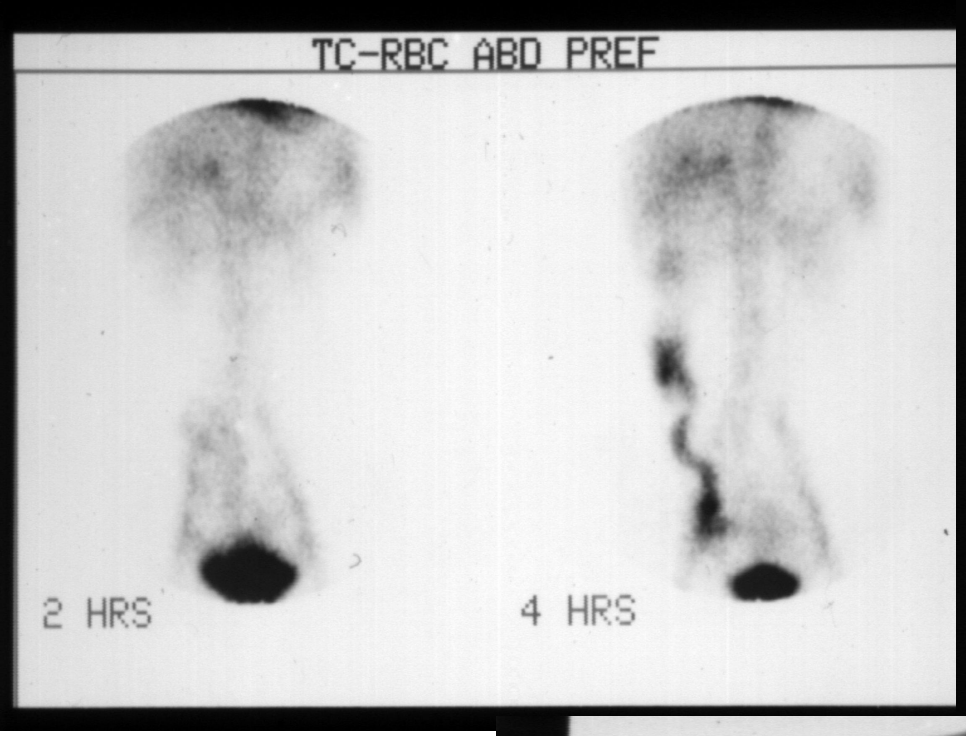
TC-RBC ABD PREF
2 HRS
4 HRS

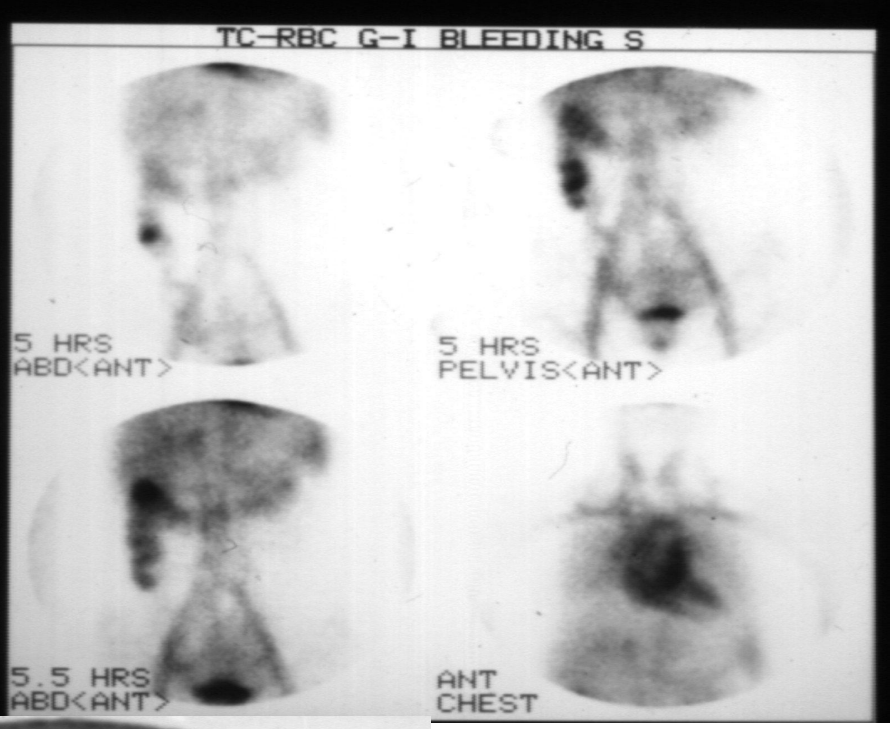
TC-RBC G-I BLEEDING S
5 HRS
ABD<ANT>
5 HRS
PELVIS<ANT>
5.5 HRS
ABD<ANT>
ANT
CHEST

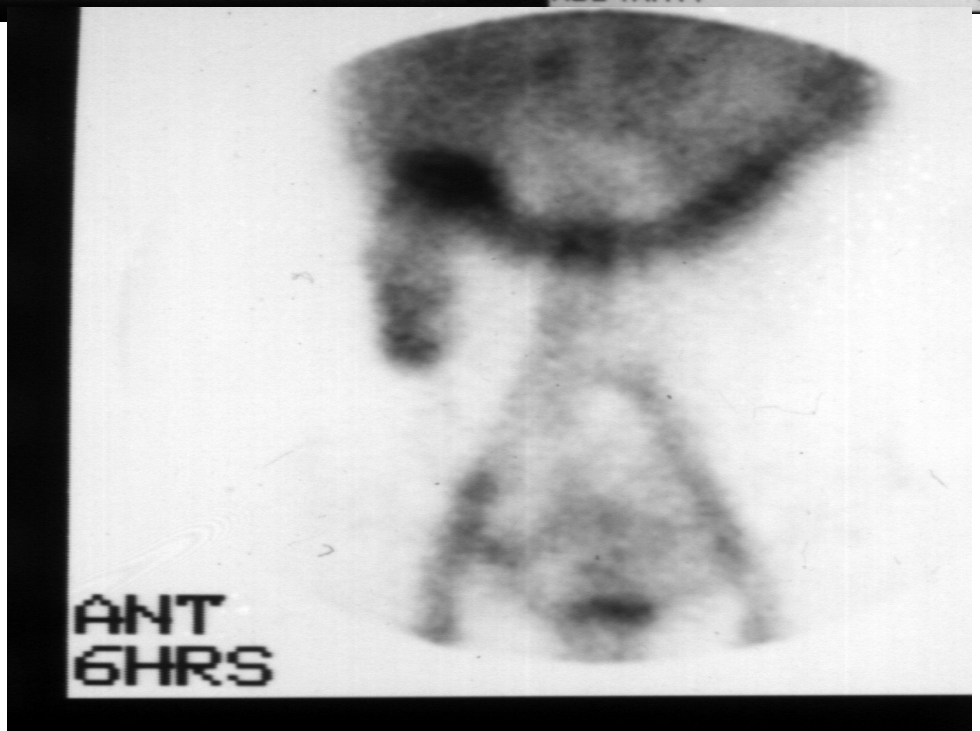
ANT
6HRS

Angiography

Nuclear imaging

- Therapy can be performed at the same setting, such as using intra-arterial vasopressin, coils or Gelfoam to stop bleeding

Angiography

Nuclear imaging

- Only 10-20% as sensitive for the evaluation of GI bleeding as is nuclear imaging

Angiography

- Can image bleeding at rates of 0.5-1 ml/min or greater

Nuclear imaging

- Image bleeding at rates as low as 0.05-0.1 ml/min

Angiography

- Will detect bleeding only if extravasation is occurring during the injection of contrast

Nuclear imaging

- May detect bleeding that can occur intermittently over a prolonged period of time after injection of the radiopharmaceutical

Angiography

- More costly
- A small risk of morbidity and mortality

Nuclear imaging

- Inexpensive
- Safe and effective

Nuclear imaging, especially the RBC-labeled study, is an excellent first-line examination

If no bleeding is identified with an RBC study even on delayed images, studies indicate these patients do well with conservative therapy and outpatient endoscopic/barium evaluation

Some angiographers insist on a positive nuclear imaging study before angiography is undertaken because of

- The increased sensitivity of the bleeding scan
- Its ability to help guide the angiographic procedure

Acute GI bleeding flowchart